UNIVERSIDADE D
COIMBRA

Jessica Gonçalves da Silva

Evaluation of the Immunotoxicological Properties of PLA Nanoparticles

Dissertação no âmbito do Mestrado em Biotecnologia Farmacêutica orientada pela Professora Doutora Olga Maria Fernandes Borges Ribeiro e co-orientada por Doutora Sandra Cristina Campos de Jesus e apresentada à Faculdade de Farmácia da Universidade de Coimbra.

Julho de 2019

1 2 9 0

UNIVERSIDADE D
COIMBRA

EVALUATION OF THE IMMUNOTOXICOLOGICAL PROPERTIES OF PLA NANOPARTICLES

Jessica Gonçalves Da Silva

Tese no âmbito do Mestrado em Biotecnologia Farmacêutica, orientada pela Professora Doutora Olga Maria Fernandes Borges Ribeiro, co-orientada pela Doutora Sandra Cristina Campos de Jesus e apresentada à Faculdade de Farmácia da Universidade de Coimbra.

Julho de 2019

The experimental work presented in this thesis was developed under the scientific supervision of Professor Doctor Olga Maria Fernandes Borges Ribeiro from the Pharmaceutical Technology Laboratory of the Faculty of Pharmacy, from the University of Coimbra, Portugal.

This work was financed by the European Regional Development Fund (ERDF), through the Centro 2020 Regional Operational Programme under project CENTRO-01-0145-FEDER-000008:BrainHealth 2020, and through the COMPETE 2020 - Operational Programme for Competitiveness and Internationalization and Portuguese national funds via FCT – Fundação para a Ciência e a Tecnologia, I.P., under project PROSAFE/0001/2016, and the strategic projects POCI-01-0145-FEDER-030331 and POCI-01-0145-FEDER-007440 (UID/NEU/04539/2019).

The authors thank Dra. Ana Donato for expertise and assistance in hemocompatibility studies in the Clinical Analysis Laboratory of the Faculty of Pharmacy of Coimbra University (Portugal), Prof. Dr. Manfred Zinn for the determination of the exact MW of PDLLA by gel permeation chromatography/ size exclusion chromatography in the University of Applied Sciences and Arts Western Switzerland (HES-SO // Valais – Wallis) and Dr. Mónica Zuzart for the TEM microscopy analyses that were performed at iLAB - Bioimaging Laboratory of the Faculty of Medicine of the University of Coimbra.

UNIÃO EUROPEIA
Fundo Europeu
de Desenvolvimento Regional

FCT
Fundação para a Ciência e a Tecnologia
MINISTÉRIO DA CIÊNCIA, TECNOLOGIA E ENSINO SUPERIOR

Acknowledgements / Agradecimentos

"A perseverança é o que torna o impossível possível, o possível provável e o provável realizado."

Léon Trotsky

Uma dissertação de mestrado consiste numa longa viagem, que inclui inúmeros desafios, incertezas, percalços, assim como alegrias e tristezas, e esta não poderia chegar a bom porto sem o precioso apoio de várias pessoas. Desta forma, gostaria de exprimir os meus sinceros agradecimentos a todos aqueles que, direta ou indiretamente, me ajudaram a concluir mais uma etapa da minha vida.

À minha orientadora, a Professora Doutora Olga Maria Fernandes Borges Ribeiro, agradeço pela oportunidade de realização de todo o trabalho no seu laboratório, assim como a sua orientação, a sua disponibilidade e todos os conhecimentos transmitidos.

À minha co-orientadora, a Doutora Sandra Jesus, agradeço por todo o apoio fornecido, pelos conselhos preciosos, pela disponibilidade e pela leitura crítica e atenta da minha dissertação de mestrado.

A toda a equipa do "nanolab", em especial à minha parceira de mestrado Natália Bernardi, assim como à Mariana Colaço, à Alana Duarte, ao João Costa, à Patrícia Marques e à Edna Soares não esquecendo, contudo, muitos outros colegas que passaram pelo laboratório e também me acompanharam neste trabalho, agradeço pelo companheirismo e disponibilidade que demonstraram durante toda esta etapa de aprendizagem no laboratório.

A todos os que trabalham no piso 4 da Faculdade de Farmácia da Universidade de Coimbra, agradeço pela disponibilidade em ajudar que sempre demonstraram.

À Faculdade de Farmácia da Universidade de Coimbra, agradeço pela oportunidade de enriquecer os meus conhecimentos e de adquirir novas competências na área da investigação científica.

Aos meus amigos, em especial à Ana Rita, à Bárbara, à Maria, à Ana Carina, à Andreia e ao Filipe, agradeço pelo vosso apoio, pela vossa paciência para me aturar, pela força que me transmitiram para continuar e nunca desistir, e, sobretudo, por todos os momentos partilhados, tanto pelos bons como pelos maus. Muito obrigada.

Por fim, mas não menos importante, aos membros da minha família, em especial aos meus pais e irmãos, agradeço pelo amor, apoio infalível e encorajamento contínuo que depositaram em mim, sem os quais não teria sido possível chegar a cabo desta longa viagem. Obrigada por possibilitarem sempre a realização dos meus sonhos. Do fundo do coração.

Table of contents

List of Tables

List of Figures

List of Abbreviations

API	Active pharmaceutical ingredient
ASTM	American society for testing and materials international
BCA	Bicinchoninic acid
BSA	Bovine serum albumin
CHI	Chitosan
CMH	Cyanmethemoglobin
ConA	Concanavalin A
CSE	Control standard endotoxin
DCFH-DA	Dichlorofluorescein diacetate probe
DD	Deacetylation degree
DLS	Dynamic light scattering
DMEM	Dulbecco's modified eagle medium
DMSO	Dimethyl sulfoxide
ELISA	Enzyme-linked immunosorbent assay
ELS	Electrophoretic light scattering
EMEA	European Medicines Evaluation Agency
FBS	Fetal bovine serum
FDA	Food and drug administration
FITC	Fluorescein isothiocyanate
GPC/SEC	Gel permeation chromatography/ size exclusion chromatography
GRAS	Generally Recognized as Sage
IL-6	Interleukin-6
ISO	International Organization for Standardization
LA	Lactic acid
LAL	Limulus amoebocyte lysate
LC	Loading capacity
LE	Loading efficacy
LPS	Lipopolysaccharide
LSCM	Laser scanning confocal microscope
MTT	3-(4,5-dimethylthiazol-2-yl)-2,5-diphenyltetrazolium bromide
MW	Molecular weight
NMR	Nuclear magnetic resonance
NO	Nitric oxide

NP	Nanoparticle
OD	Optical density
PBMC	Peripheral blood mononuclear cell
PBS	Phosphate-buffered saline
PCL	Polycaprolactone
PDI	Polydispersity index
PDLA	Poly(D-lactide)
PDLLA	Poly(D,L-lactide)
pI	Isoelectric point
PI	Propidium iodide
PLA	Polylactic acid
PLGA	Poly(lactic-co-glycolic acid)
PLLA	Poly(L-lactide)
pNA	Para-nitroaniline
PVA	Polyvinyl alcohol
ROP	Ring opening polymerization
ROS	Reactive oxygen species
RPMI	Roswell Park Memorial Institute medium
RT	Room temperature
SD	Standard deviation
SEM	Standard error of the mean
TBH	Total blood hemoglobin
TBHd	Total blood hemoglobin diluted
TEM	Transmission electron microscopy
TNF- α	Tumor necrosis factor-α
VC	Vehicle control

Abstract

Polylactic acid (PLA) is a FDA-approved biodegradable and biocompatible polymer derived fully from renewable resources, which has been widely used as a promising nanoparticulate delivery system. However, when used as a polymeric nanoparticle (NP), its immunotoxicological effects are not well-documented. Thus, this study intends to evaluate the toxicity of two different sized PLA NPs (PLA_A NPs and PLA_B NPs) after extensive physicochemical characterization in *in vitro* experimental conditions. Additionally, another two polymeric NPs were produced and used as terms of comparison: polycaprolactone (PCL) NPs and PCL/chitosan (PCL/CHI) NPs.

After production, PLA_A NPs mean diameter (187.9 ± 36.9 nm) was superior to PLA_B NPs (109.1 ± 10.4 nm). Concerning the other polymeric NPs, PCL/CHI NPs presented a mean diameter (266.1 ± 63.8 nm) superior to PCL NPs (170.0 ± 15.2 nm) and a distinctive positive zeta potential, confirming the presence of CHI in the NP structure. However, when dispersed in cell culture media, all NPs presented different sizes, which we may explain their behavior in the assays performed.

For instance, contrary to what was previously assessed in pyrogen-free water, in DMEM medium, PLA_A NPs presented smaller mean diameter when compared to PLA_B NPs, which may explain its higher toxicity in RAW 264.7, presenting an estimated IC_{50} of 540.6 μg/mL. The same happened with PCL/CHI NPs, which size drastically decreased in DMEM medium, and showed the highest toxicity among all NP tested, with an estimated IC_{50} of 68.89 μg/mL. Likewise, PLA_A and PCL/CHI NPs were also the ones that induced a significant concentration-dependent ROS production.

Irrespective of size differences, none of the polymeric NPs of this study, in concentrations tested, presented an inflammatory potential (NO production) in RAW 264.7, nor toxicity in PBMCs or hemolytic activity in human blood.

Concerning cytokines release (TNF-α and IL-6) from human PBMCs, the presence of CHI in the PCL/CHI NPs structure seemed to exacerbate cytokines release when compared to PCL NPs. Nonetheless, both presented a higher increase of cytokines release when compare with PLA NPs. However, despite the use of 6 different blood donors, these results need to be repeated with more donors due to the great variability verified between individuals. Also, although the NPs are produced in endotoxin-free conditions, this study could be repeated in presence of polymyxin B, to guarantee that if any LPS was present in samples, its effect would be mitigated.

Moreover, NPs ability to act as protein delivery systems was confirmed through protein adsorption assays with three model proteins (bovine serum albumin (BSA), myoglobin and lysozyme), followed by cell uptake studies in PBMCs using NPs adsorbed with the BSA-FITC model protein.

Overall, the results suggest that PLA NPs are hemocompatible without causing inflammatory reactions and that PLA NPs presenting a smaller sized population possess increased cytotoxicity and ability to induce ROS production.

Furthermore, this study emphasizes the importance of interpreting results based on adequate physicochemical characterization of the nanoparticulate delivery systems in biological media, since small differences in size triggered by the dispersion in cell culture media can be related to the differences on the cytotoxicity. If not accounted for, these differences can lead to misinterpretations, and subsequent ambiguous conclusions.

Keywords: polylactic acid (PLA), polycaprolactone (PCL), chitosan (CHI), polymeric nanoparticles, immunotoxicological profile.

Resumo

O ácido polilático (PLA) é um polímero biodegradável e biocompatível aprovado pela FDA derivado de recursos renováveis, o qual tem sido amplamente utilizado como um promissor sistema de entrega nanoparticulado. No entanto, quando usado como nanopartícula polimérica (NP), os seus efeitos imunotoxicológicos não se encontram bem documentados. Assim sendo, este estudo pretende avaliar a toxicidade de duas NPs de PLA com tamanhos diferentes (PLA_A NPs e PLA_B NPs) após uma extensa caracterização físico-química em condições experimentais *in vitro*. Adicionalmente, outras duas NPs poliméricas foram produzidas e usadas como termos de comparação: as NPs de policaprolactona (PCL) e as NPs de PCL/quitosano (PCL/CHI).

Após produção, o diâmetro médio das NPs de PLA_A (187,9 nm ± 36,9 nm) foi superior às NPs de PLA_B (109,1 nm ± 10,4 nm). Em relação às outras NPs poliméricas, as NPs de PCL/CHI apresentaram um diâmetro médio (266,1 nm ± 63,8 nm) superior às NPs de PCL (170,0 nm ± 15,2 nm) e um potencial zeta positivo distinto das outras NPs, confirmando desta forma a presença de CHI na estrutura da NP. No entanto, quando dispersas em meio de cultura celular, todas as NPs apresentaram um perfil diferente, o que poderá explicar os resultados dos ensaios realizados.

Por exemplo, contrariamente ao que foi observado anteriormente em água apirogénica, em meio DMEM, as NPs de PLA_A apresentaram um diâmetro médio menor quando comparado com o tamanho das NPs de PLA_B, o que pode explicar a respetiva maior toxicidade observada em RAW 264.7, apresentando um IC_{50} estimado de 540,6 µg/mL. O mesmo aconteceu com as NPs de PCL/CHI, as quais também apresentaram um decréscimo no tamanho em meio DMEM e foram as que apresentaram maior toxicidade, com um IC_{50} estimado de 68,89 µg/mL. Da mesma forma, as NPs de PLA_A e PCL/CHI induziram os níveis dependentes da concentração usada mais elevados de produção de espécies reativas de oxigénio (ROS).

Independentemente das diferenças de tamanho, nenhuma das NPs poliméricas deste estudo apresentou um potencial inflamatório (produção de NO) em RAW 264,7, nem toxicidade em PBMCs ou ainda atividade hemolítica em sangue humano.

Relativamente à produção de citocinas (TNF-α and IL-6), a presença de CHI na estrutura das NPs de PCL/CHI pareceu exacerbar a produção de citocinas quando comparadas às NPs de PCL mas ambas levaram a um aumento maior de produção de citocinas quando comparadas com as NPs de PLA. No entanto, apesar de terem sido usados sangues de 6 dadores diferentes, estes resultados deveriam ser repetidos com mais dadores devido à variabilidade

entre indivíduos. Ademais, apesar das NPs serem produzidas em condições livres de endotoxinas, este estudo poderia ser repetido na presença de polimixina B, de forma a garantir que, se algum LPS estiver presente nas amostras, os seus efeitos sejam mitigados.

Além disso, a capacidade das NPs de atuarem como sistemas de entrega de fármacos foi confirmada através de ensaios de adsorção de proteínas com três proteínas modelo (albumina de soro bovino (BSA), mioglobina e lisozima), seguidos de estudos de uptake em PBMCs usando NPs com a proteína modelo BSA-FITC adsorvida à superfície.

De forma geral, os resultados sugerem que as NPs de PLA são hemocompatíveis sem causarem reações inflamatórias e que as NPs de PLA que apresentam uma população de menor tamanho possuem uma citotoxicidade aumentada e capacidade para induzir a produção de ROS.

Desta forma, este estudo enfatiza a importância da interpretação dos resultados com base numa caracterização físico-química adequada dos sistemas de entrega nanoparticulados em meios biológicos, uma vez que pequenas diferenças de tamanho desencadeadas pela dispersão nestes meios de cultura celular podem ter repercussões na toxicidade. Se não forem tidas em conta, estas diferenças podem levar a interpretações erradas e conclusões ambíguas.

Palavras-chave: Ácido poliláctico (PLA); policaprolactona (PCL); quitosano (CHI); nanopartículas poliméricas; perfil imunotoxicológico.

Chapter 1 – Introduction

1.1 Nanotechnology – some definitions

When talking about nanotechnology, it is important to establish some definitions, in order to avoid misinterpretations between the researchers and the readers. Therefore, here are some important definitions in the field of nanotechnology.

First of all, what is nanotechnology? The term nanotechnology has different definitions according to different regulatory authorities. For instance, the reflection paper on Nanotechnology-based Medicinal Products for Human Use (EMEA/CHMP/79769/2006) from the European Medicines Evaluation Agency (EMEA) defined nanotechnology as "the production and application of structures, devices and systems by controlling the shape and size of materials at nanometer scale, being that the nanometer scale, or nanoscale, ranges from the atomic level at around 0.2 nm (2 Å) up to around 100 nm" (EMEA, 2006), whereas the guidance document on Considering Whether an FDA-Regulated Product Involves the Application of Nanotechnology (FDA-2010-D-0530) from the Food and Drug Administration (FDA) defined products that involve the application of nanotechnology as "products that contain or are manufactured using materials with dimensions up to 1000 nm, as well as products that contain or are manufactured using certain materials that otherwise exhibit related dimension-dependent properties or phenomena" (FDA, 2014). Considering these definitions, it is common to address the nanoscale up to around 1000 nm in the scientific literature.

Another important term to define is nanomaterial, which is defined by the International Organization for Standardization (ISO) as "a material with any external dimensions in the nanoscale or having internal structure or surface structure in the nanoscale" (ISO/TC229, 2015a). It may include: nano-objects, defined as "discrete pieces of material with one, two or three external dimensions in the nanoscale", and nanostructured materials, defined as "materials having internal nanostructure or surface nanostructure". Nano-objects, in their turn, may include nanoplates, nanofibers and nanoparticles (NPs). The first one is defined as a "nano-object with one external dimension in the nanoscale and the other two external dimensions significantly larger", the second one as "a nano-object with two external dimensions in the nanoscale and the third dimension significantly larger", and the third one as "a nano-object with all external dimensions in the nanoscale where the lengths of the longest and the shortest axes of the nano-object do not differ significantly" (ISO/TC229, 2015b).

NPs have been widely used as promising drug delivery systems, because of their versatile properties provided by their small size. In fact, some of their advantages include the

protection of the active pharmaceutical ingredient (API), as well as its site specific and controlled delivery (de Faria, T.J., Machado de Campos, A. and Lemos Senna, E., 2005, Hirsjärvi, S., 2008, Moorkoth, D. and Nampoothiri, K.M., 2014). Furthermore, NPs can be presented in different forms as illustrated in Figure 1.1, polymeric NPs being the ones that will be the object of study of this dissertation.

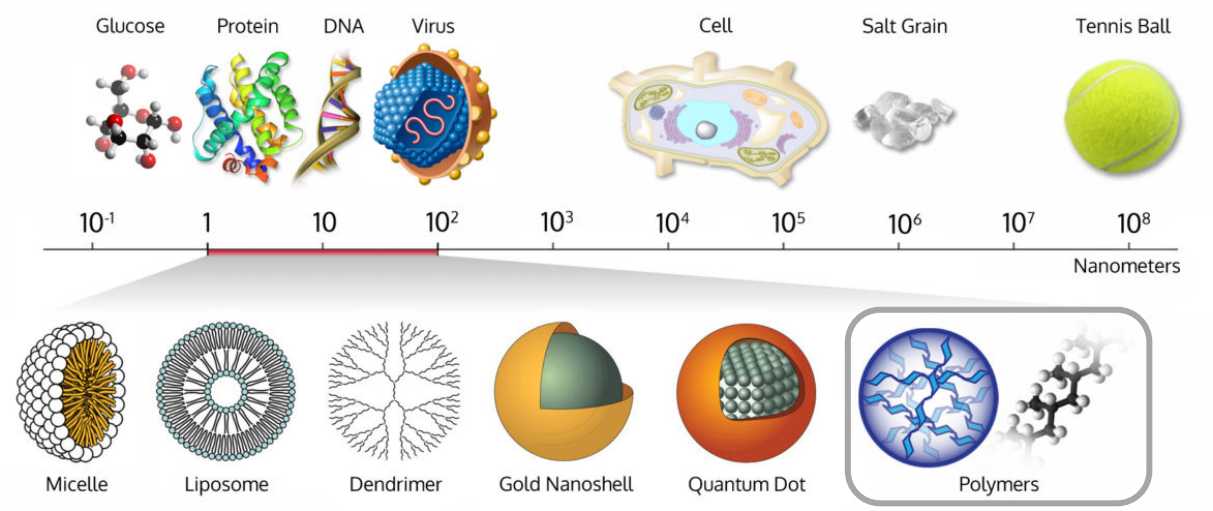

Figure 1. 1 – Nanometer scale and the different types of nanoparticles. Adapted from: (WichResearchLab, 2017).

1.2 Polymeric Nanoparticles

Polymeric NPs have been shown to be one of the most promising vehicles that can help to overcome hurdles in formulation science. One example of that is Abraxane®, which was the first polymeric nanoparticulate product approved by FDA in 2005. This nanoparticulate system consists of albumin-bound paclitaxel nanoparticles and is free of the toxic solvent cremophor-EL, which was previously used to solubilize paclitaxel for intravenous (IV) administrations and was known to cause life-threatening allergic reactions (Castro, E. and Kumar, A., 2013). Therefore, Abraxane® showed to be a successful drug delivery system of paclitaxel, since it overcame the side effects of the IV administration. Actually, the use of polymeric NPs may include several advantages, such as the increase of the stability of any API and the decrease of the costs associated with their production, since they can be cheaply fabricated in large scale (Castro, E. and Kumar, A., 2013).

Several polymers can be used for the production of polymeric nanoparticulate systems, including natural and synthetic polymers. Some examples of natural polymers are gelatin, chitosan (CHI), albumin and alginate, however, their use may involve some inherent disadvantages, such as poor batch-to-batch reproducibility, tendency to degrade and

potential for antigenicity. An alternative may be the use of synthetic polymers, such as different polyesters (polycaprolactone (PCL) and poly(lactic acid) (PLA) (Castro, E. and Kumar, A., 2013).

PLA is derived fully from renewable resources and, therefore, is one of the most abundant FDA-approved biodegradable polymers (Moorkoth, D. and Nampoothiri, K.M., 2014). Correspondingly, PLA will be the focus of this dissertation as a polymeric nanoparticulate system (PLA NPs) and will be compared with other two polymeric NPs: PCL and PCL/CHI NPs.

1.2.1 PLA Nanoparticles

Poly(lactic acid) (PLA) is one of the most extensively investigated member of the aliphatic polyester family regarding many therapeutic applications (Nair, L.S. and Laurencin, C.T., 2007). Its chemical structure is represented in the right side of Figure 1.2. As mentioned above, PLA is considered as a Generally Recognized as Safe (GRAS) material by FDA and has proven to be a very versatile material with interesting properties (Castro-Aguirre, E. *et al.*, 2016, Farah, S.Anderson, D.G. and Langer, R., 2016). It has a glass transition temperature around 55 to 59 °C and a melting point of 174 – 184 °C (Lasprilla, J. *et al.*, 2011). PLA can be obtained by two major methods: direct polycondensation of lactic acid (LA) and ring opening polymerization (ROP) of lactide, the lactic acid cyclic dimmer, as represented in Figure 1.2 (Castro-Aguirre, E. *et al.*, 2016, Farah, S., Anderson, D.G. and Langer, R., 2016, Gupta, B., Revagade, N. and Hilborn, J., 2007, Lasprilla, J. *et al.*, 2011, Murariu, M. and Dubois, P., 2016).

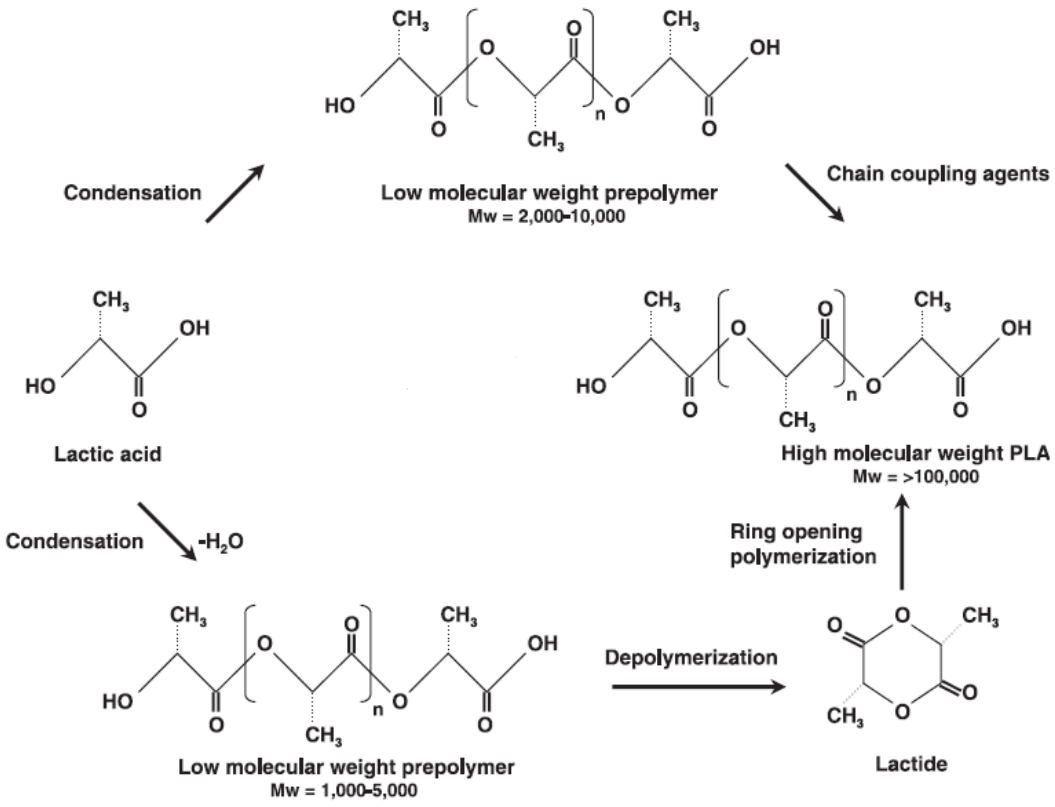

Figure 1. 2 – Schematic representation of PLA synthesis methods. Retired from: (Lasprilla, J. *et al.*, 2011).

LA, the basic block of PLA, is a simple chiral molecule, which can be presented in the form of two optically active enantiomers, L- and D-lactic acid, causing PLA to have different stereoisomers, such as poly(L-lactide) (PLLA), poly(D-lactide) (PDLA), and poly(D,L-lactide) (PDLLA). PDLLA is an amorphous polymer, due to the random distribution of L- and D-lactide units, showing a much lower strength (~ 1.9 GPa) compared to PLLA. PDLLA having a faster degradation rate and a lower strength when compared to PLLA, it is a preferred candidate for drug delivery and tissue regeneration applications (Farah, S., Anderson, D.G. and Langer, R., 2016, Lasprilla, J. *et al.*, 2011, Nair, L.S. and Laurencin, C.T., 2007, Tsuji, H., 2016, Tyler, B. *et al.*, 2016).

Furthermore, PLA exhibits several advantages, including biocompatibility, biodegradability, non-toxicity, bioabsorbability, thermoplastic processability and energy-savings production. Thus, PLA has been explored regarding many biomedical applications. Despite its advantages, PLA also presents some drawbacks, including poor toughness, slow degradation rate, hydrophobicity and lack of reactive side-chain groups. These weaknesses limit its use in certain applications (Farah, S., Anderson, D.G. and Langer, R., 2016). All in considered, PLA still remains an encouraging candidate for several biomedical applications.

Additionally, despite initially being limited to medical application, such as implant devices, tissue scaffolds, internal sutures and others, due to its high cost and low availability, high MW PLA can now be processed by cheaper methods and, thus, has been a promising alternative to petrochemical-based synthetic polymers (Castro-Aguirre, E. *et al.*, 2016, Murariu, M. and Dubois, P., 2016). Accordingly, we choose PLA as a suitable nanoparticulate delivery system, deserving more attention in order to be a well-standardized polymer regarding the evaluation of its immunotoxicological profile.

1.2.2 PCL Nanoparticles

Poly(ε-caprolactone) (PCL) is another member of the aliphatic polyester family and its chemical structure is represented in the right side of Figure 1.3. This hydrophobic, semi-crystalline polymer is of great interest as it presents several advantages. In fact, one of its advantages is the fact that it can be obtained of a relatively cheap monomeric unit "ε-caprolactone" by ROP, as represented in Figure 1.3 (Nair, L.S. and Laurencin, C.T., 2007).

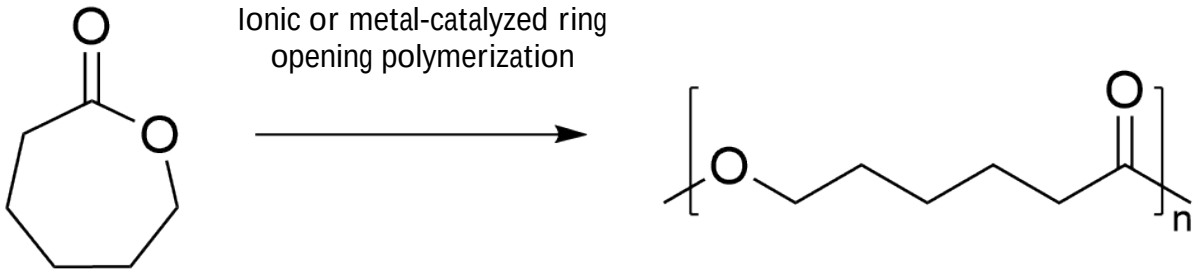

ε-caprolactone poly(ε-caprolactone)

Figure 1. 3 – chematic representation of ring opening polymerization of ε-caprolactone. Adapted from: (Labet, M. and Thielemans, W., 2009).

It has a low melting point (55–60 °C) and glass transition temperature (-60 °C) (Fuoco, T. and Finne-Wistrand, A., 2019, Nair, L.S. and Laurencin, C.T., 2007). Some other advantages include that it is highly processible, due to its solubility in a wide range of organic solvents, it has an excellent biocompatibility and despite is low tensile strength (~ 23 MPa), it has an extremely high elongation at breakage (> 700 %) (Nair, L.S. and Laurencin, C.T., 2007). In addition to its non-toxicity, PCL has a slow degradation rate, which means that it has the ability to be investigated as a long-term drug/vaccine delivery vehicle, in opposition to PLA. However, numerous co-polymeric systems containing PCL have also been investigated, in order to improve its inherent properties (Nair, L.S. and Laurencin, C.T., 2007, Woodruff,

M.A. and Hutmacher, D.W., 2010). An example of that is a co-polymer of PCL and CHI, as will be discussed below.

1.2.3 PCL/CHI Nanoparticles

Chitosan (CHI) is a natural polymer, which can be obtained from chitin through enzymatic or chemical processes, chemical conversion being preferred due to its suitability for mass production and lower cost. In fact, alkaline deacetylation of chitin allows us to obtain CHI, which is formed by D-glucosamine and N-acetyl-D- glucosamine units, linked by β-1,4 glycosidic linkages, each one chemical structure being represented in Figure 1.4 (Muxika, A. *et al.*, 2017).

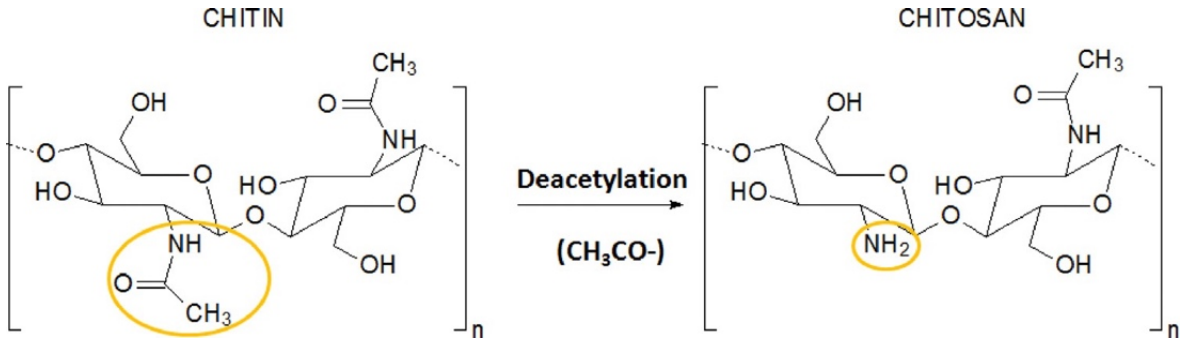

Figure 1. 4 – Schematic representation of alkaline deacetylation of chitin and chemical structure of chitin and chitosan. Retired from: (Muxika, A. *et al.*, 2017).

CHI is a mucopolysaccharide being more and more investigated in pharmaceutical and biomedical fields, due to its versatile properties. Actually, CHI has an excellent biocompatibility, biodegradability and low toxicity (Kulkarni, A.D. *et al.*, 2017). Moreover, CHI has a low solubility in neutral and alkaline media (Kulkarni, A.D. *et al.*, 2017, Muxika, A. *et al.*, 2017), but it is soluble in aqueous acidic media when its deacetylation degree reaches about 50 %. When dissolved in acidic media, this polymer acquires a positive charge, due to the protonation of its amino groups in the chain. This property is thought to be responsible for its antimicrobial activity, since this positive charge may interact with the negatively charged membranes of microorganisms (Muxika, A. *et al.*, 2017). Besides this biomedical application, many others can be attributed to CHI in the biomedical field, due to its many benefits, such as controlled drug delivery, wound dressing, tissue engineering, blood anticoagulant and bone regeneration biomaterial. However, being a natural polymer, CHI presents some inherent disadvantages, such as poor batch-to-batch reproducibility, tendency to degrade and potential for antigenicity, as mentioned above (Castro, E. and Kumar, A.,

2013). To deal with these drawbacks, CHI can be combined to a synthetic polymer, such as PCL, in order to improve their inherent disadvantages and take advantage of each one benefits. Thus, this co-polymer will be used in this dissertation as another nanoparticulate delivery system, in order to assess it advantages, or not, when compared to mono-nanoparticulate system of PCL and both nanoparticulate systems will be paralleled to PLA NPs.

1.3 Importance of Immunotoxicological Studies

Polymeric NPs are promising delivery systems, that are being used more and more in a variety of applications. They can both enter the body unintentionally or be intentionally administered to the body for biomedical applications. Inside the body, it has been shown that NPs have the potential to interact with the immune system by stimulating or suppressing immune responses, for instance through the binding to proteins in the blood (Dobrovolskaia, M.A. and McNeil, S.E., 2007, Kononenko, V.Narat, M. and Drobne, D., 2015). Therefore, it is important to evaluate NP toxicity in the immune system (immunotoxicity) and, despite generally regarded as safe, the polymeric NP immunotoxicological effects are not well documented. Furthermore, there is no clear understanding of the mechanisms that may be involved to account for widely differing immunological effects. Overall, there is an urgent need to standardize experimental procedures to assess NP immunotoxicity, in order to allow the establishment of regulations about the health risk assessment evaluation of nanoparticles.

Figure 1. 5 – Schematic representation of the biodistribution of NPs and their correspondent target sites of immunotoxicity.

1.4 *In Vitro* Tests for the Evaluation of the Immunotoxicological Effects of Nanoparticles

Currently, besides the existence of international guidelines for other materials such as the international ISO 10993-1:2018 – "Biological evaluation of medical devices" (ISO, 2018), there is no specific guideline for the assessment of toxicity and biocompatibility of nanomaterials. Nevertheless, we can rely on these guidelines for the assessment of toxicity and biocompatibility of nanomaterials.

Different systems of the human body may be included for the evaluation of NP immunotoxicological effect such as the circulatory system and the immune system. Accordingly, we proposed the use of three different models: human blood, murine macrophage RAW 264.7 cell line and peripheral blood mononuclear cells (PBMCs).

Concerning the different assays to be performed, for the evaluation of NP hemocompatibility profile, hemolysis, as well as coagulation and platelet aggregation assays may be performed, as recommended in part 4 of ISO 10993 – "Selection of tests for interactions with blood". In its turn, the evaluation of NP immunocompatibility profile may include assays with the macrophage RAW 264.7 cell line, such as cytotoxicity, reactive oxygen species (ROS) production, nitric oxide (NO) production and inhibition, and cytokines release, and assays with PBMCs, such as cytotoxicity, proliferation and cytokines release, as recommended by part 1 of ISO 10993 – "Evaluation and testing within a risk management process".

1.5 Immunotoxicological Studies – State-of-the-Art

Although the interest in polymeric nanoparticles has been growing more and more, as well as their use, the evaluation of their immunotoxicity is not well documented and even less standardized. Nonetheless, we found several articles in the literature, performing one or another assay proposed for such evaluation. The different articles found are listed in Table 1.1 and will be used throughout the text as comparison terms for the discussion of the results of the different assays performed.

Table 1. 1 - Review of original articles assessing the toxicity of polymeric nanoparticles, including PLA, PCL, PCL/CHI or CHI nanoparticles, using the following endpoints: hemolysis, cytotoxicity, inflammation and oxidative stress.

Nanomaterial	Polymer characterization	Nanomaterial characterization	Endpoint	Testing method	Model	Dose/concentration range	Results	Reference
Tamoxifen loaded PLA NPs	85–160 kDa PLA	155 nm - 21.7 mV	Hemolysis	Erythrocyte incubation (4, 12, 24,48, 72, 96 h)	Human blood	4.4 µM or 1.1 µM of tamoxifen	Negligible hemolysis at both concentrations and all incubations times	**(Altmeyer, C. *et al.*, 2016)**
PLA NPs	na	176 nm – 58 mV In cell culture: 212 nm – 24 mV	Oxidative stress	2′,7′-Dichlorofluorescin diacetate (DCF-DA) probe (72 h)	Schneider's Drosophila melanogaster line 2 (S2) cells	0.5 - 500 µg/mL	ROS production was only observed at the highest tested concentration (500 µg/mL) indicating a concentration dependent effect	**(Legaz, S. *et al.*, 2016)**
PLA NPs	DL-PLA (MW 10000)	256 nm - 17.1 mV	Oxidative stress	2′,7′-Dichlorofluorescin diacetate (DCF-DA) probe (24 h)	RAW 264.7 cells	10, 30, 100 and 300 µg/mL	No effect on ROS production up to 100 µg/ml concentration; 300 µg/ml showed 1.5- to 2-fold stimulation of ROS production	**(Singh, R.P. and Ramarao, P., 2013)**
			Inflammation	*In vitro* cytokine production (24 h)		300 µg/mL	No induction of the IL-6 release; 1.5- to 2-fold increase in TNF-α release	
PCL NPs	PCL (intrinsic viscosity 1.07g/dl)	268 nm –9.10 mV	Oxidative stress	2′,7′-Dichlorofluorescin diacetate (DCF-DA) probe (24 h)		10, 30, 100 and 300 µg/mL	No effect on ROS production up to 100 µg/ml concentration; 300 µg/ml showed 1.5- to 2-fold stimulation of ROS production	
			Inflammation	*In vitro* cytokine production (24 h)		300 µg/mL	No induction of the IL-6 release; 1.5- to 2-fold increase in TNF-α release	
PCL/CHI NPs	PCL (MW 14000) Low molecular weight chitosan (95 % DD)	539.1 nm + 21.7 mV	Cytotoxicity	*In vitro* cytotoxicity with PBMCs	Human blood	40 µg/mL	Cell viability decrease of almost 50 %	**(Jesus, S. *et al.*, 2017)**
Chitosan NPs	270 kDa	367 nm + 5 mV	Hemolysis	Erythrocyte incubation (2 h)	Human blood	2000 µg/mL	Chitosan NPs were slightly hemolytic (~ 7 %)	**(Shelma, R. and Sharma, C.P., 2011)**
Chitosan NPs	Low molecular weight chitosan (85 % DD)	≤100 nm + 40 mV	Hemolysis	Erythrocyte incubation (2 h)	Human blood	50-300 µg/mL	No significant hemolysis	**(Sarangapani, S. *et al.*, 2018)**

Chitosan stabilized PLGA NPs	75:25 Resomer® RG756 and Protasan® UP CL113,75–90% deacetylation, 50–150 kDa	Ratio chi:PVA:PLGA 15.3:30.4:100 230 nm +40 mV	Inflammation	In vitro cytokine production (24 h)	A549 and THP-1-D cell co-culture	0.1 mg/mL or 1m g/mL	Mild inflammatory response to PLGA nanoparticles stabilized by the hydrophilic polymer chitosan slightly higher than the stabilizer-free PLGA nanoparticles	**(Grabowski, N. *et al.*, 2016)**
Chitosan stabilized PLGA NPs	75:25 Resomer® RG756 and Protasan® UP CL113,75–90% deacetylation, 50–150 kDa	Ratio chi:PVA:PLGA 15.3:30.4:100 230 nm + 40 mV (270 nm in cell culture medium)	Inflammation	In vitro cytokine production (24h)	THP-1 cell culture	0.1 mg/mL or 1 mg/mL	0.1 mg/mL and 1 mg/mL did not induce cytokine secretion[1]	**(Grabowski, N. *et al.*, 2015)**
Chitosan NPs	Low molecular weight chitosan (85 % DD)	≤100 nm + 40 mV	Oxidative stress	Dichlorofluorescin diacetate (DCF-DA) probe (na h)	BCL2(AAA) Jurkat cells	10-50 µg/mL	Concentration dependent ROS production	**(Sarangapani, S. *et al.*, 2018)**
Chitosan NPs	na	164 nm; + 63 mV 385 nm; + 62 mV 459 nm; +72 mV 475 nm; +71 mV 685 nm; +74 mV	Oxidative stress	Dihydroethidium (DHE) probe (72 h)	Mouse bone marrow-derived hematopoietic stem cells	250-1000 µg/mL	ROS production was not significantly altered following exposure to chitosan NPs.	**(Omar Zaki, S.S.Katas, H. and Hamid, Z.A., 2015)**
Chitosan NPs	75-85 % 50-190 kDa	173 nm + 23 mV	Oxidative stress	Dichlorofluorescin diacetate (DCF-DA) probe (24 h)	HEK-293 cells	100 µg/mL	Chitosan NPs had no effect on ROS production	**(Arora, D. *et al.*, 2016b)**
Chitosan NPs	80 % DD 400 kDa	100 nm + 19 mV	Oxidative stress	Dichlorofluorescin diacetate (DCF-DA) probe (6/12/24 h)	Hela and SMMC-7721 cells	10 or 100 µg/mL	Chitosan NPs increase ROS production in a concentration-dependent manner	**(Wang, H. *et al.*, 2018)**

[1] According to the authors, IL-6 levels were not statically different from the control but neither were LPS levels. Considering this, chitosan stabilized PLGA NPs induced IL-6 levels similar to LPS.

From the analysis of Table 1.1, we observed that there are a lot of disparities between authors. For instance, both Legaz and co-workers as well as Singh and Ramarao evaluated the oxidative stress caused by PLA NPs with DCF-DA probe, the first ones observing only an effect at 500 µg/mL, while the seconds observed an effect at 300 µg/mL. However, they performed the assay with a different model, Schneider's Drosophila melanogaster line 2 (S2) cells for Legaz and co-workers and RAW 264.7 cells for Singh and Ramarao. Furthermore, Legaz and co-workers did not specify which isoform of PLA was used in their experiments.

Another example of such disparities was the assessment of oxidative stress caused by CHI NPs. Despite using the same probe, Sarangapani *et al.*, Arora *et al.* and Wang *et al.* performed the assay with different cellular models between them and all referred different results. Also, all of them tested different NP concentrations. Importantly, the ones who tested the higher concentrations may be having a NP associated toxicity influencing, in this way, the obtained results. Moreover, we can observe that CHI NPs produced by the different authors have different physicochemical properties and this could be one possible reason for the different results.

One last example was the evaluation of the CHI NPs hemocompatibility profile. For that, both Shelma and Sharma as well as Sarangapani *et al.* performed hemolysis assays through the incubation of CHI NPs with human erythrocytes for 2 h, however they tested different concentration ranges which lead to different conclusions. Additionally, once again, CHI NPs produced by the different authors presented different physicochemical properties, possibly leading to some differences in the respective hemocompatibility profile.

In fact, disparities were present both in the testing method used, in the model used or even in the concentration range tested.

Therefore, more than highlighting the ambiguous results found by the different authors, this table stresses the need to develop standardized procedures for the assessment of NP immunotoxicological effects.

1.6 Aim of the Work

As described above, polymeric NPs are promising nanoparticulate delivery systems, but their immunotoxicological effects are not well documented. Thus, this study intends to contribute to fill this gap, by proposing diverse objectives:

- To develop and optimize two different methods to produce two different sized PLA NPs;
- To optimize a method to produce PCL and PCL/CHI NPs;

- To perform a broad characterization of the different polymeric NPs produced in pyrogen-free water and in the different cell culture media used;
- To evaluate the immunotoxicological effects of PLA NPs in a detailed way and to compare it between the two different sized PLA NPs;
- To analogize it with the immunotoxicological profile of two other polymeric NPs: PCL and PCL/CHI NPs, and to understand the effect of CHI presence in PCL-based NPs;
- To relate NPs characteristics with its immunotoxicity, ultimately addressing for toxicity trends.

Chapter 2 – Development and/or optimization of a method to produce the different polymeric nanoparticles and their characterization

Adapted from: DA SILVA, J., S. JESUS, N. BERNARDI, *et al.* Poly(D,L-Lactic Acid) Nanoparticle Size Reduction Increases Its Immunotoxicity. **Frontiers in Bioengineering and Biotechnology,** 2019, 7. DOI: 10.3389/fbioe.2019.00137.

2.1 Materials and Methods

2.1.1 Polymers

2.1.1.1 Poly(D,L-Lactide)

Poly(D,L-lactide) (PDLLA) polymer with an average molecular weight (MW) of 75 000 Da to 120 000 Da and an inherent viscosity of 0.55 dL/g to 0.75 dL/g was obtained from Sigma-Aldrich Corporation (St. Louis, MO, USA). The exact MW of PDLLA was 101 782 Da determined after analysis by gel permeation chromatography/ size exclusion chromatography (GPC/SEC).

2.1.1.2 Poly-ε-caprolactone

Poly-ε-caprolactone (PCL) polymer with an average molecular weight (MW) of ~14 000 Da and a viscosity of 400 mPa.s to 1000 mPa.s (50 wt. % in xylene) was obtained from Sigma-Aldrich Corporation (St. Louis, MO, USA).

2.1.1.3 Chitosan

Chitosan (CHI) polymer with an average molecular weight (MW) of 164 kDa and a degree of deacetylation (DD) of 75 % after purification was obtained from Primex BioChemicals AS (Avaldsnes, Norway). The DD of chitosan was determined after purification by nuclear magnetic resonance (NMR) as previously described in (Lavertu, M. *et al.*, 2003).

2.1.2 Development and Optimization of the Method to Produce PLA_A nanoparticles

2.1.2.1 Nanoparticle Production and Concentration

For PLA_A nanoparticle (NP) production, PDLLA was dissolved at 2 mg/mL in acetone. NPs formed spontaneously upon dropwise addition of 4.5 mL of PDLLA solution to 13.5 mL of an aqueous solution with 1 % of Pluronic® F68 Prill (Basf Corporation, Ludwigshafen, Germany) using a high-speed homogenizer at 13000 rpm as represented in Figure 2.1. The homogenization was maintained for another 2 min, after total addition of the PDLLA solution (Da Silva, J. *et al.*, 2019).

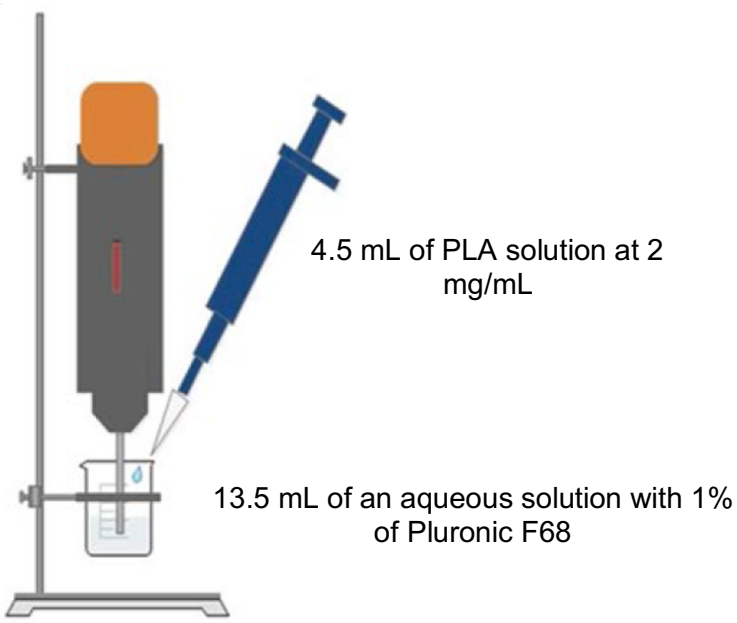

Figure 2. 1 – Schematic representation of the method of production of PLA_A NPs. Adapted from: (Jesus, S., Soares, E. and Borges, O., 2016).

The PLA_A NPs suspended in the original medium were concentrated by centrifugation at 13000 g for 20 min at 10 °C, resuspended in pyrogen-free water and concentrated again. This procedure was repeated 2 more times, and finally each batch was concentrated in a final volume of 2 mL at a concentration of 2250 µg/mL (Da Silva, J. *et al.*, 2019). This final concentration was determined after the yield of NP production of 50 % $\pm$ 5.5 % was obtained upon lyophilization, through the following equation (eq. 1):

$$Yield\ of\ production\ (\%) = \frac{mass\ of\ lyophilized\ NPs\ (mg) \times final\ volume\ of\ each\ batch\ (mL)}{theoretical\ mass\ of\ polymers\ added\ in\ each\ batch\ (mg) \times lyophilized\ volume\ (mL)}\ x\ 100 \qquad \text{(eq. 1)}$$

2.1.3 Development and Optimization of the Method to Produce PLA_B nanoparticles

2.1.3.1 Nanoparticle Production and Concentration

On the other hand, for the production of smaller PLA NPs, named PLA_B NPs, we reduced the polymer concentration used for the NP production as well as the percentage of surfactant and we also changed the method of homogenization and the method of centrifugation. In fact, PDLLA was dissolved at 0.75 mg/mL in acetone and NPs formed spontaneously upon dropwise addition of 1 mL of PDLLA solution to 2.5 mL of an aqueous

solution with 0.1 % of Pluronic F68 using a vortex homogenizer as exemplified in Figure 2.2. The agitation was maintained for another minute, after the total addition of the PDLLA solution (Da Silva, J. *et al.*, 2019).

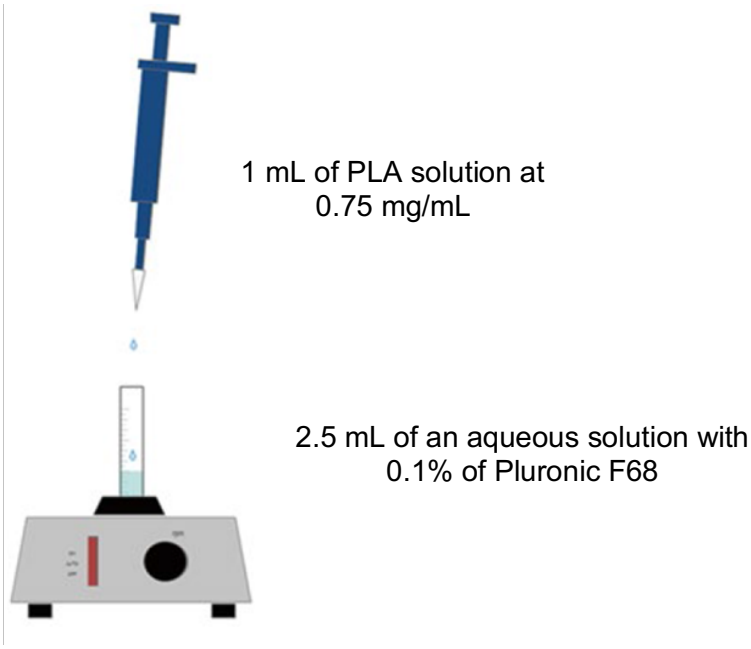

Figure 2. 2 – Schematic representation of the method of production of PLA_B NPs. Adapted from: (Jesus, S., Soares, E. and Borges, O., 2016).

In order to concentrate and wash the NPs, 8 batches of PLA_B NPs (20 mL) were centrifuged with Vivaspin 20 centrifugal concentrator (MWCO 300KD, ThermoFisher Scientific Inc., Waltham, MA, USA) at 3000 g at 10 °C until less than 1 mL was recovered in the centrifuge tube. The NPs were then resuspended in 10 mL pyrogen-free water, the centrifugation procedure was repeated, and the NPs were resuspended in a final volume of 1 mL pyrogen-free water at a final concentration of 4286 µg/mL (Da Silva, J. *et al.*, 2019). This final concentration was determined after the yield of NP production of 100 % $\pm$ 8.8 % was obtained upon lyophilization, through equation 1.

2.1.4 Optimization of the Method to Produce PCL nanoparticles

2.1.4.1 Nanoparticle Production and Concentration

For PCL NPs production, a previously described method by our group was chosen. Briefly, PCL was dissolved at 0.2 % in acetone (Jesus, S. *et al.*, 2018). NPs formed spontaneously upon dropwise addition of 4.5 mL of PCL solution to 13.5 mL of a solution of acetic acid at 0.1 % with 5 % of Tween 80® from (Riedel de Haen™, Seelze, Germany) using a high-speed

homogenizer at 13000 rpm. The homogenization was maintained for another minute, after total addition of the PCL solution.

For the optimization of NP concentration procedure, the starting point chosen was a centrifugation at 16000 g for 20 min at 20 °C and from there, the force of centrifugation was increased as well as the time of centrifugation. In fact, we tested which of these two forces of centrifugation: 16000 g and 21000 g and which of these two times of centrifugation: 20 min and 60 min were better to concentrate the NPs. To choose between these parameters, we evaluated the supernatants transmittance, allowing us to choose the better method of concentration and a consequent better yield of production. All this in mind, the method chosen was the concentration by centrifugation at 16000 g for 60 min at 20 °C of PCL NPs suspended in the original medium, the resuspension in pyrogen-free water and concentration again. This procedure was repeated 2 more times, and finally each batch was concentrated in a final volume of 2 mL at a concentration of 3600 µg/mL. This final concentration was determined after the yield of NP production of 80 % $\pm$ 8.3 % was obtained upon lyophilization, through equation 1.

2.1.5 Optimization of the Method to Produce PCL/CHI nanoparticles

2.1.5.1 Nanoparticle Production and Concentration

As for PCL NPs production, for PCL/CHI NPs production, a previously described method by our group was chosen (Jesus, S. *et al.*, 2018). In short, PCL (0.2 %) was dissolved in acetone. NPs formed spontaneously upon dropwise addition of 4.5 mL of PCL solution to 13.5 mL of a solution of chitosan (0.1 %) in acetic acid at 0.1 % with 5 % of Tween 80® from (Riedel de Haen™, Seelze, Germany), left dissolving overnight, using a high-speed homogenizer at 13000 rpm. The homogenization was maintained for another minute, after total addition of the PCL solution.

The method of concentration of PCL/CHI NPs was also optimized as described before for PCL NPs. Hence, the PCL/CHI NPs suspended in the original medium were also concentrated by centrifugation at 16000 g for 60 min at 20 °C, resuspended in pyrogen-free water and concentrated again. This procedure was repeated 2 more times, and finally each batch was concentrated in a final volume of 2 mL at a concentration of 3000 µg/mL. This final concentration was determined after the yield of NP production of 27 % $\pm$ 3.0 % was obtained upon lyophilization, through equation 1.

2.1.6 NPs Characterization

Zetasizer Nano ZS (Malvern Instruments, Ltd., Worcestershire, UK) was used to measure particle size, and the respective polydispersity index (PDI), by dynamic light scattering (DLS) and particle zeta potential through electrophoretic light scattering (ELS). The samples were characterized dispersed in pyrogen-free water and in supplemented culture media (Roswell Park Memorial Institute medium - RPMI and Dulbecco's Modified Eagle Medium - DMEM). In the second case, the size and zeta potential assessment was done immediately after dilution in the culture medium, and after 24 h of incubation at 37 °C. The NP size when dispersed in pyrogen-free water was also confirmed by transmission electron microscopy (TEM). Samples were placed on a microscopy grid and observed under a FEI-Tecnai G2 Spirit Biotwin, a 20–120 kV TEM (FEI Company, OR, USA) (Da Silva, J. *et al.*, 2019).

2.1.7 Protein adsorption assay

In order to evaluate the capacity of the different NPs to adsorb model therapeutic proteins on its surface, adsorption studies with three different proteins (bovine serum albumin (BSA), myoglobin and lysozyme) were performed. Bovine serum albumin (BSA, 96 % fraction V), Myoglobin from equine skeletal muscle (95 % to 100 %), Lysozyme (≥ 80 %) were purchased from Sigma Aldrich Corp. (St Louis, MO, USA). For that, all NPs were incubated at 500 µg/mL with different concentrations of the different proteins for 1 h under rotational agitation, then they were centrifuged for 30 min at 21000 g and 25 µL of the supernatants were collected for non-bound protein quantification. Pierce™ Bicinchoninic acid (BCA) protein assay, purchased from Thermo Fisher Scientific Inc. (Waltham, MA, USA) was performed in microplates (Pierce Chemical Company, Rockford, IL, USA).

To analyze the obtained results, it is fundamental to understand and be able to distinguish two terms: Adsorption efficacy and nanoparticle adsorption capacity. The Adsorption efficacy (AE (%)) is defined as the percentage of protein that is successfully adsorbed on the surface of the NP and is calculated using the following equation (eq. 2):

$$Adsorption\ efficacy\ (\%) = \frac{total\ amount\ of\ protein\ added - free\ non{-}bound\ protein}{total\ amount\ of\ protein\ added} x\ 100$$

(eq. 2)

On its side, the nanoparticle adsorption capacity (AC (%)) is the amount of protein adsorbed per unit of weight of the NP and is calculated using the following equation (eq. 3):

$$Nanoparticle\ adsorption\ capacity\ (\%) = \frac{total\ amount\ of\ protein\ (\mu g/mL) - free\ non-bound\ protein(\mu g/mL)}{NP\ weight\ (\mu g/mL)}\ x\ 100 \qquad \text{(eq. 3)}$$

2.1.8 Statistical analysis

Data were analyzed using GraphPad Prim 6 (GraphPad Software, Inc., La Jolla, CA, USA), in which significant differences were obtained from one-way ANOVA, and values were considered statistically different when $p < 0.05$. Data were expressed as means ± standard deviation (SD) or standard error of the mean (SEM) for protein adsorption assays.

2.2 Results and Discussion

2.2.1 All nanoparticles were efficiently produced using a simple and reproducible nanoprecipitation method

In order to study the immunotoxicological profile of the different NPs produced and to establish a comparison between them, the first step was to optimize the preparation methods in order to obtain:

1 - PLA NPs with two different sizes (PLA_A and PLA_B NPs) in order to study the influence of the size on the immunotoxicological profile of the PLA NP.

2 - PCL NPs and CHI coated PCL NPs (PCL and PCL/CHI NPs) in order to study the effect of the presence of the CHI on the immunotoxicological profile of PCL nanoparticles, and to use these two NPs as terms of comparison for PLA NPs.

The preparation method of the PLA NPs was settled after the analysis of the methods described in scientific literature which were summarized in Table 2.1.

Table 2. 1 – Summary of the methods found in the literature that helped to establish and optimize a method for the production of PLA NPs.

Reference	PLA polymer	Production method	Size (nm)	Zeta potential (mV)
(Fessi, H. *et al.*, 1989)	Poly-(D,L-lactide) polymer	Interfacial polymer deposition + solvent displacement	229 nm ± 29 nm	/
(Sambandam, B. *et al.*, 2015)	Poly D-L lactide (Mw= 75 000 Da to 120 000 Da), Sigma-Aldrich	Nanoprecipitation method + rotary evaporator	185 nm ± 10 nm	-20.5 mV ± 1.0 mV
(de Faria, T.J.Machado de Campos, A. and Lemos Senna, E., 2005)	Poly(D,L-lactide), Boehringer Ingelheim	Interfacial deposition process + filtered through 0.8 μm cellulose ester membranes	251.9 nm	-33.2 mV ± 0.5 mV
(Moorkoth, D. and Nampoothiri, K.M., 2014)	Poly (L-Lactic Acid) (Mw=85 000 kDa to 160 000 kDa), Sigma	Double emulsion solvent evaporation	128 nm ± 15 nm (sonication time=5min) 112 nm ± 6 nm (sonication time=20 min)	-11.0 mV -15.4 mV
(Pandey, S.K. *et al.*, 2015)	Poly(D,L-Lactic Acid) (Mw ~ 120 000 Da), Biomer, Germany	Emulsified (o/w) nanoprecipitation method + ultracentrifugation	32 nm ± 8 nm to 153 nm ± 9 nm from 10 mg/ml to 40 mg/ml of PLA concentration	/

The nanoprecipitation method to produce the PLA NPs proposed by Sambandam *et al.* (Sambandam, B. *et al.*, 2015) was adopted in this work by two reasons. First, the polymer that was used was similar to the one we had (Sigma-Aldrich, Mw 75 000 Da to 120 000 Da). Second, the characteristics of the NPs produced by Sambandam *et al.* were similar to the ones that we wanted to obtain. However, some modifications were introduced to the method. Briefly, the polyvinyl alcohol (PVA) surfactant was replaced by Pluronic® F68 Prill and the homogenization was performed at 13 000 rpm. After these modifications, we managed to produce our PLA_A NPs by a simple and reproducible nanoprecipitation method.

On the other hand, for the production of the smaller PLA NPs (PLA_B NPs) we tried to reduce the polymer concentration as well as the percentage of surfactant and we also changed the method of homogenization and of centrifugation, as described in more detail in section 2.1.3. With these adjustments, we succeeded in producing smaller PLA NPs (PLA_B NPs) also by a simple and reproducible nanoprecipitation method.

Concerning PCL and PCL/CHI NPs, a previously described method by our group was chosen, since it was a simple and reproducible nanoprecipitation method too. In this case, only the concentration and washing steps were optimized as described in 2.1.4.1 and 2.1.5.1.

The NPs were then characterized regarding their mean particle size, size distribution, PDI and zeta potential when dispersed in pyrogen-free water. Results are presented in Figure 2.3.

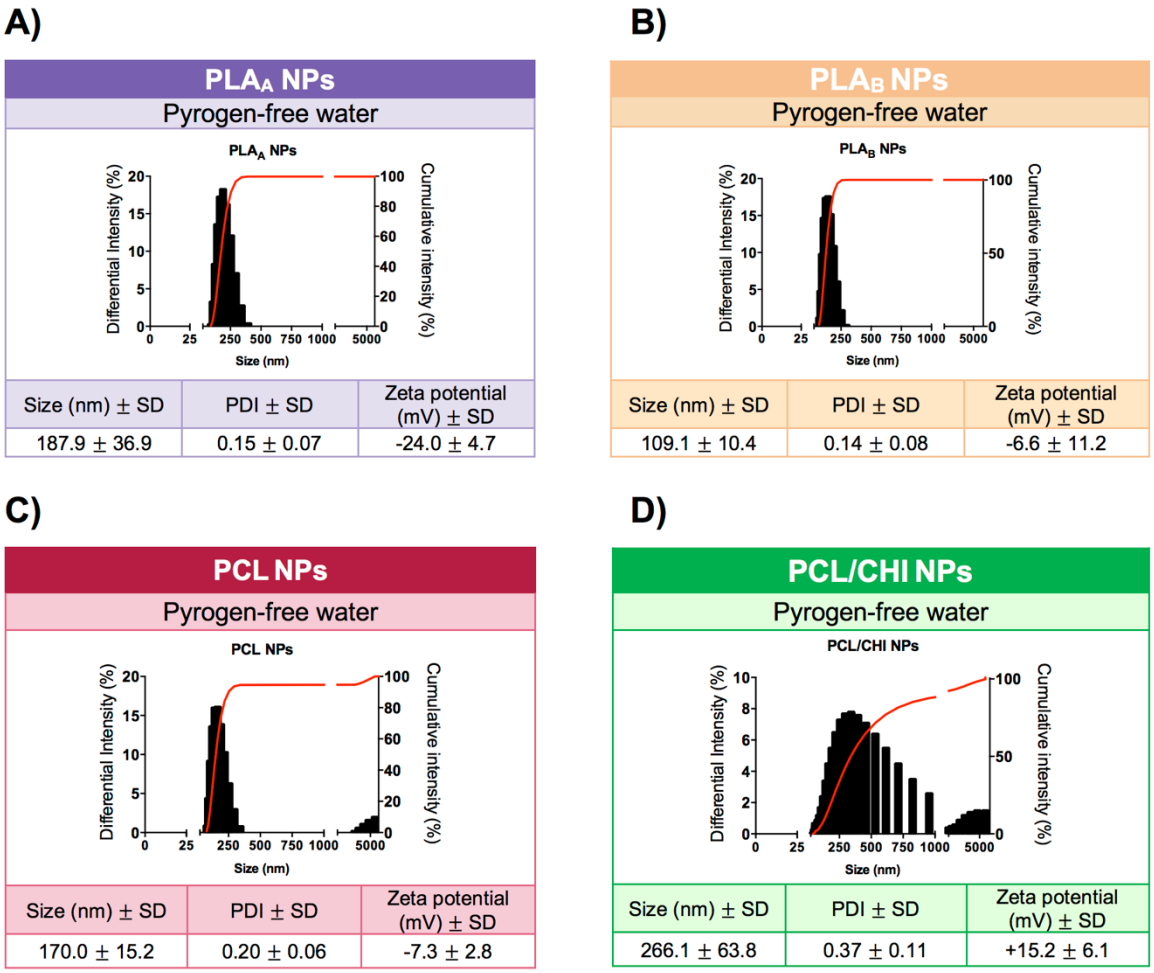

Figure 2. 3 – NPs Characterization. Particle mean size distribution (nm), polydispersity index (PDI), zeta potential (mV) and illustrative graphics of differential and cumulative intensities, after concentration and resuspension in pyrogen-free water. A) PLA_A NP. B) PLA_B NP. C) PCL NP. D) PCL/CHI NP. Data are presented as mean ± standard deviation (SD), n≥3 (three or more independent experiments, each in triplicate).

PLA_A NPs presented a mean diameter of 187.9 nm and a zeta potential of -24.0 mV in pyrogen-free water, while PLA_B NPs presented a smaller mean diameter of 109.1 nm and a more neutral zeta potential of -6.6 mV, both presenting PDI compatible with only one narrow-size population of particles (see distribution size graphic on Figure 2.3A and B). The more negative charge of PLA_A NPs could be explained by the higher concentration of Pluronic F68 used in the NP production, since increased surface layer of surfactant may decreases the NPs zeta potential (Santander-Ortega, M.J. *et al.*, 2006). On their turn, PCL NPs presented a mean diameter similar to the one of PLA_A NPs, of 170.0 nm and an almost neutral zeta potential of -7.3 mV. PCL/CHI NPs were the larger NP in this study, with a mean diameter of 266.1 nm and a distinctive positive zeta potential of +15.2 mV. The larger mean diameter of the PCL/CHI NPs is also accompanied by a larger PDI, meaning a more heterogeneous size population, well illustrated by the size dispersion graph (Figure 2.3D). This last result can be explained by the presence of CHI, which shows propensity to form agglomerates in aqueous media (Karchiyappan, T. and Prasad, R., 2019). Due to the presence of this second polymer (CHI) in the PCL/CHI NP structure, these NPs also present a distinctive positive zeta potential. In fact, when in acidic solution, CHI polymer is known to confer a positive charge (Illum, L. *et al.*, 2001). Concerning the PDI of PCL NPs, it is low, compatible with an homogenous size population of particles, however it is higher than the PLA NPs PDI, and the size dispersion graphs confirm the existence of a small population of aggregates (Figure 2.3C).

2.2.2 Transmission Electron Microscopy (TEM) confirmed NPs size and their round shaped morphology

The NP size and morphology were also evaluated through a TEM analysis. Samples dispersed in pyrogen-free water were dried on a microscopy grid prior to observation and the images obtained are represented in Figure 2.4.

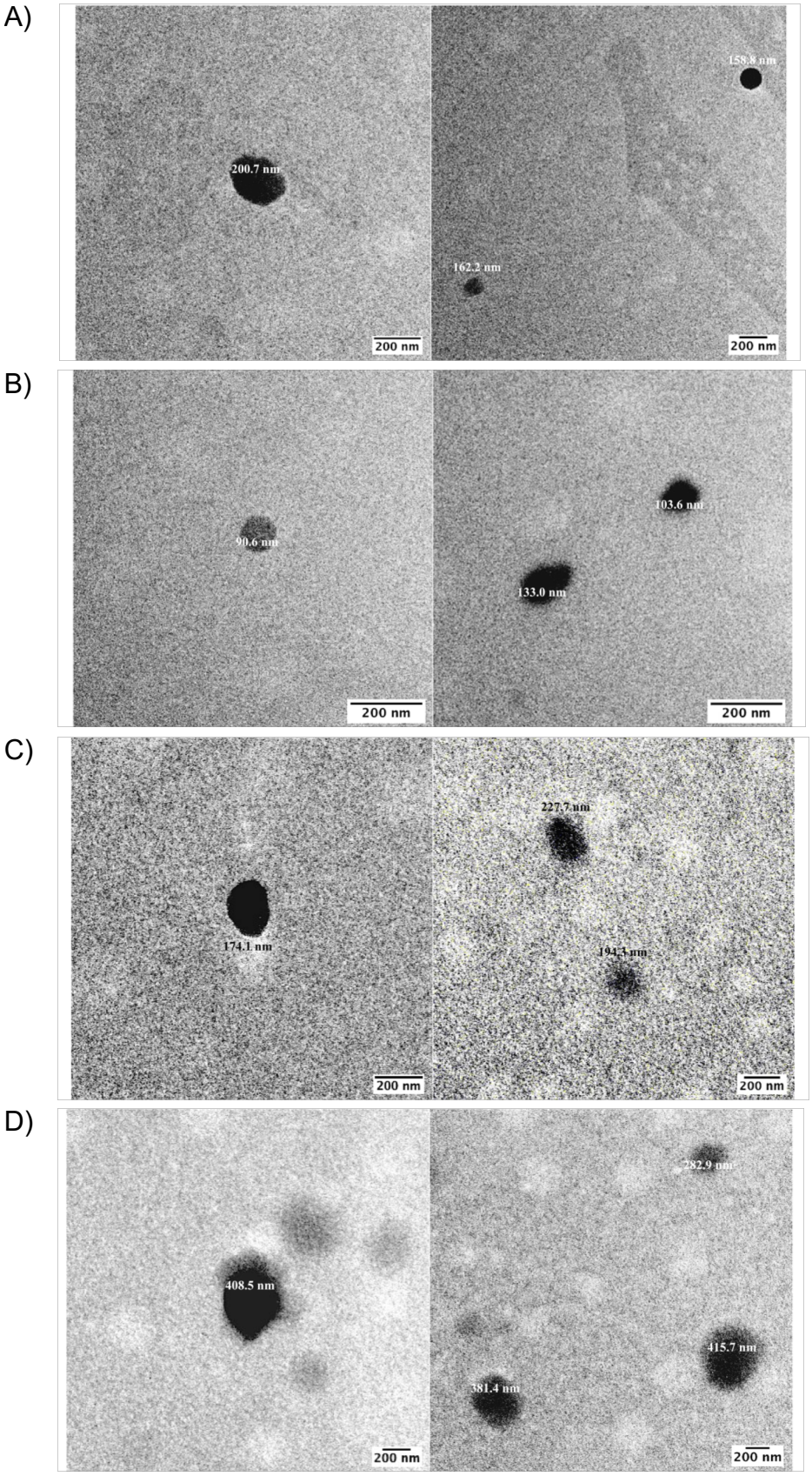

Figure 2. 4 – TEM images of the different NPs dispersed in pyrogen-free water (scale bar: 200 nm) A) PLA_A NPs. B) PLA_B NPs. C) PCL NPs. D) PCL/CHI NPs.

The PLA_A NPs presented a rounded shape, with sizes ranging between 158.8 and 200.7 nm, as exemplified in Figure 2.4A. These sizes are concordant with the mean diameter obtained from DLS. When analyzing Figure 2.4B, we can observe that PLA_B NPs also presented a rounded shape, however with smaller sizes ranging between 90.6 and 133.0 nm, which likewise corresponds with the mean diameter obtained from DLS.

About PCL NPs, they also presented a rounded shape and sizes similar to the ones obtained for PLA_A NPs, ranging between 174.1 and 227.7 nm (Figure 2.4C). Here again, these sizes are concordant with the mean diameter obtained from DLS.

Finally, concerning PCL/CHI NPs, they also presented a rounded shape, with bigger sizes ranging between 282.9 and 415.7 nm, as we can see in Figure 2.4D. The inclusion of the second polymer in the NP structure is likely to be in the origin of the bigger sizes. Furthermore, these sizes are coincident with the mean diameter obtained from DLS and with the larger PDI of these NPs, since sizes observed in Figure 2.4D were more variable than with the other NPs.

2.2.3 NPs size distribution is highly influenced by the NPs dispersion in cell culture media

The NPs stability in the different supplemented culture media (RPMI and DMEM) was evaluated, in order to have the real perception of particle characteristics during the *in vitro* studies with cells. NPs characterization results when dispersed in pyrogen-free water were compared with the results obtained immediately after dilution in the cell culture medium, and after 24 h of incubation at 37 °C. Results are presented in Figure 2.5.

A)

PLA_A NPs

Pyrogen-free water			DMEM medium			RPMI medium		
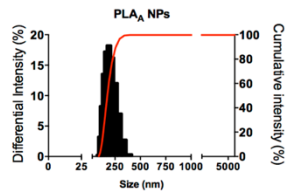			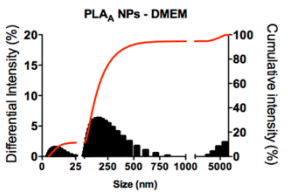			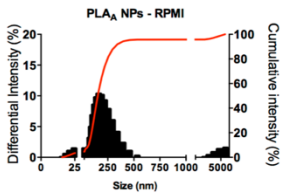		
Size (nm) ± SD	PDI ± SD	Zeta potential (mV) ± SD	Size (nm) ± SD	PDI ± SD	Zeta potential (mV) ± SD	Size (nm) ± SD	PDI ± SD	Zeta potential (mV) ± SD
187.9 ± 36.9	0.15 ± 0.07	-24.0 ± 4.7	78.3 ± 5.9 (t_0) 75.3 ± 9.8 (t_{24})	0.64 ± 0.05 (t_0) 0.69 ± 0.10 (t_{24})	-0.4 ± 0.4 (t_0) -0.9 ± 0.2 (t_{24})	92.4 ± 13.8 (t_0) 109.0 ± 20.0 (t_{24})	0.50 ± 0.01 (t_0) 0.51 ± 0.02 (t_{24})	-0.5 ± 0.3 (t_0) -0.9 ± 0.5 (t_{24})

B)

PLA_B NPs

Pyrogen-free water			DMEM medium			RPMI medium		
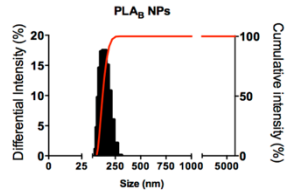			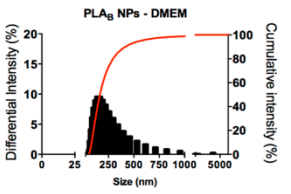			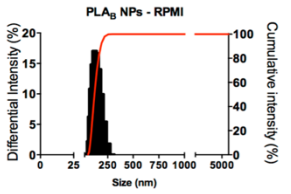		
Size (nm) ± SD	PDI ± SD	Zeta potential (mV) ± SD	Size (nm) ± SD	PDI ± SD	Zeta potential (mV) ± SD	Size (nm) ± SD	PDI ± SD	Zeta potential (mV) ± SD
109.1 ± 10.4	0.14 ± 0.08	-6.6 ± 11.2	154.1 ± 42.9 (t_0) 161.9 ± 8.2 (t_{24})	0.34 ± 0.09 (t_0) 0.37 ± 0.03 (t_{24})	-0.7 ± 0.2 (t_0) -1.0 ± 0.7 (t_{24})	182.1 ± 54.6 (t_0) 131.4 ± 15.1 (t_{24})	0.27 ± 0.09 (t_0) 0.21 ± 0.05 (t_{24})	-0.8 ± 0.3 (t_0) -0.7 ± 0.3 (t_{24})

C)

PCL NPs

Pyrogen-free water			DMEM medium			RPMI medium		
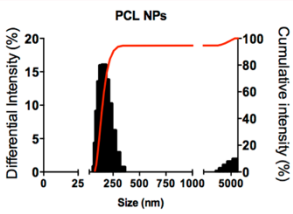			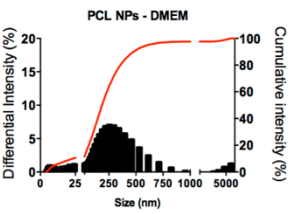			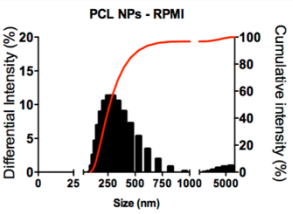		
Size (nm) ± SD	PDI ± SD	Zeta potential (mV) ± SD	Size (nm) ± SD	PDI ± SD	Zeta potential (mV) ± SD	Size (nm) ± SD	PDI ± SD	Zeta potential (mV) ± SD
170.0 ± 15.2	0.20 ± 0.06	-7.3 ± 2.8	120.4 ± 18.5 (t_0) 124.9 ± 20.1 (t_{24})	0.50 ± 0.06 (t_0) 0.72 ± 0.09 (t_{24})	-2.1 ± 2.0 (t_0) -3.4 ± 2.2 (t_{24})	178.0 ± 29.1 (t_0) 219.4 ± 44.7 (t_{24})	0.27 ± 0.02 (t_0) 0.23 ± 0.05 (t_{24})	-1.02 ± 0.7 (t_0) -2.0 ± 1.4 (t_{24})

D)

PCL/CHI NPs

Pyrogen-free water			DMEM medium			RPMI medium		
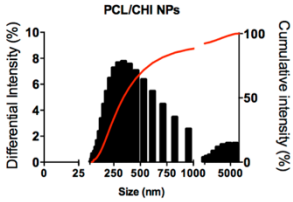			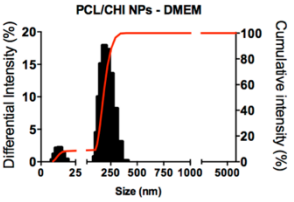			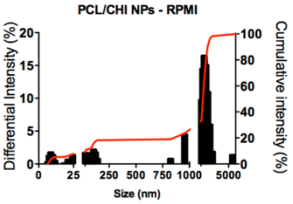		
Size (nm) ± SD	PDI ± SD	Zeta potential (mV) ± SD	Size (nm) ± SD	PDI ± SD	Zeta potential (mV) ± SD	Size (nm) ± SD	PDI ± SD	Zeta potential (mV) ± SD
266.1 ± 63.8	0.37 ± 0.11	+15.2 ± 6.1	90.2 ± 22.8 (t_0) 116.5 ± 16.7 (t_{24})	0.81 ± 0.14 (t_0) 0.59 ± 0.09 (t_{24})	-1.2 ± 0.4 (t_0) -4.4 ± 2.2 (t_{24})	173.7 ± 6.1 (t_0) 863.5 ± 93.1 (t_{24})	0.27 ± 0.01 (t_0) 0.59 ± 0.33 (t_{24})	-0.5 ± 0.2 (t_0) -1.8 ± 0.2 (t_{24})

Figure 2. 5 – Polymeric Nanoparticle Stability Tests after 24 h of incubation in cell culture media at 37 °C. Particle mean size distribution (nm), polydispersity index (PDI), zeta potential (mV) and illustrative graphics of differential and cumulative intensities, directly after resuspension in cell culture media (DMEM medium or RPMI medium) (t_0) and after 24 h of incubation (t_{24}). A) PLA_A NP. B) PLA_B NP. C) PCL NP. D) PCL/CHI NP. Data are presented as mean ± standard deviation (SD), n≥3 (three or more independent experiments, each in triplicate).

About the stability of the different NPs in the experimental assay conditions (cell culture media), with few exceptions, the results from initial dispersion and after 24 h incubation were comparable (Figure 2.5). The 24 h incubation period did not alter the characteristics of the particles. However, great differences were observed, when compared with the initial size of the particles suspended in pyrogen-free water with the particles suspended in RPMI, but especially in DMEM (Figure 2.5). In case of PLA_A NPs, the size decreased and in case of PLA_B NPs the size increased. To better understand the differences, representative graphs of differential and cumulative intensities of size distribution were obtained for the different NPs, suspended in pyrogen-free water and after 24 h incubation in RPMI and DMEM. When comparing the PLA_A graphs from cell culture media with the ones obtained in the pyrogen-free water, we observed the appearance of 3 size-populations, compatible with a higher PDI (Figure 2.5A). To highlight, the appearance of a small size population of particles explaining the decrease of the mean size diameter. The same phenomenon was not observed with PLA_B NPs. For PLA_B NPs, in RPMI the size remained unaltered and in DMEM the size increased as a result of some aggregation of the particles (Figure 2.5B).

About PCL NPs, the size decreased after 24 h incubation in DMEM and, contrariwise, remained relatively the same after 24 h incubation in RPMI. When comparing the PCL representative graphs of differential and cumulative intensities of size distribution from incubation in DMEM with the ones obtained in pyrogen-free water, the appearance of 3 size-populations was observed, compatible with a higher PDI (Figure 2.5C). To highlight, the appearance of a small size population of particles explaining the decrease of the mean size diameter, as occurred with PLA_A NPs.

Concordantly, in DMEM the same phenomenon of size reduction was observed with PCL/CHI NPs, however, only a 2 size-populations was observed, but also compatible with a higher PDI (Figure 2.5D). Importantly, for PCL/CHI NPs, a great change was observed after 24 h incubation in RPMI, since the size substantially increased. In fact, the appearance of several sized-populations was observed, and the population with higher intensity is likely to result from nanoparticle aggregation as it is superior to 1000 nm (Figure 2.5D).

2.2.4 Protein adsorption is comparable among all developed polyester NPs despite small differences

As explained above, adsorption studies with different proteins are a suitable way to evaluate the ability of the different NPs to function as antigen or therapeutic protein delivery system. For that, the different NPs were incubated at 500 µg/mL with 3 different concentrations of model proteins for 1 h. Results are presented in Figure 2.6.

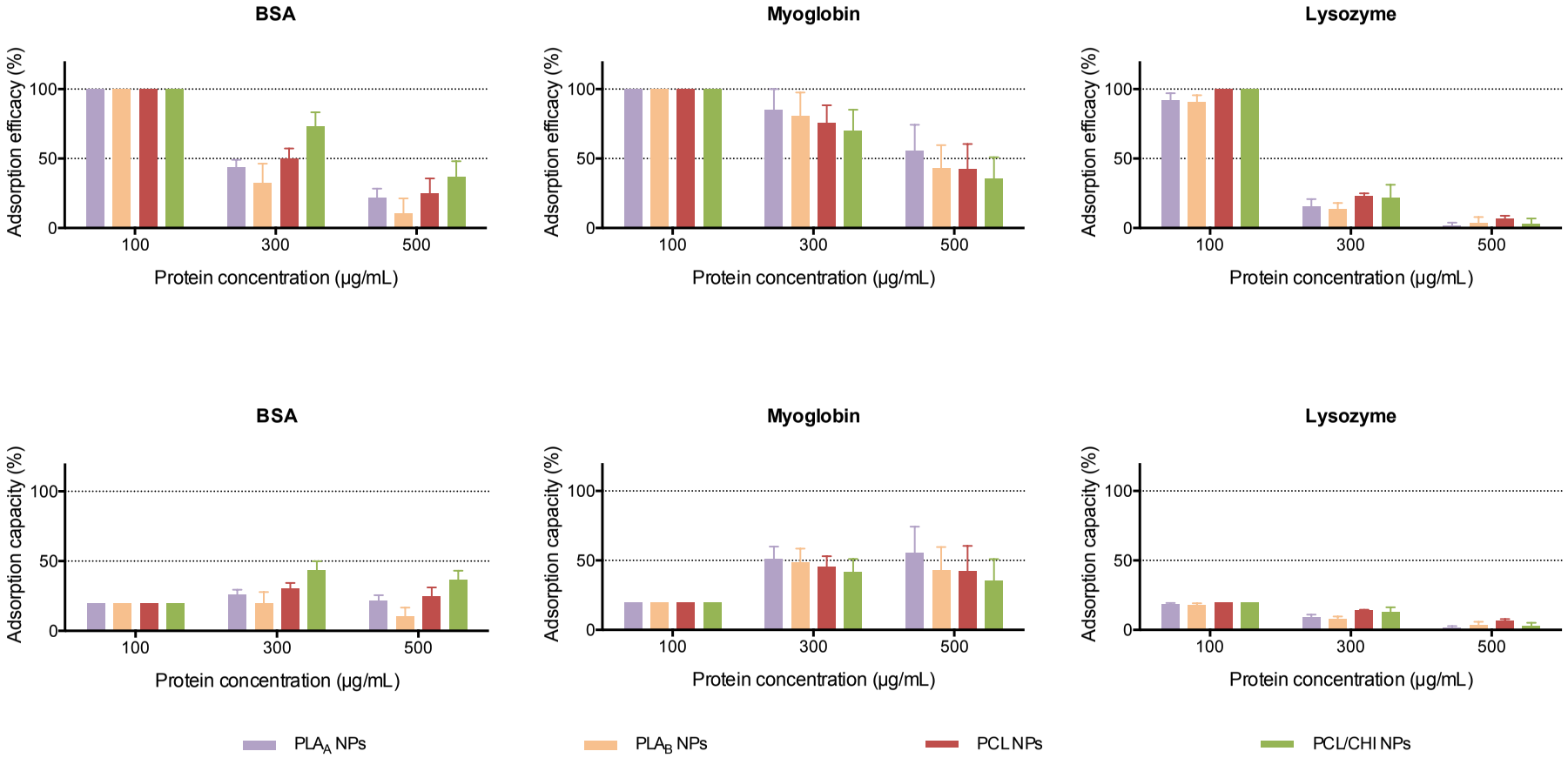

Figure 2. 6 – Protein adsorption assays after 1 h of incubation of the different NPs with BSA, myoglobin or lysozyme at room temperature (RT) under rotational agitation. Data are presented as mean ± standard error of the mean (SEM), n≥3 (three or more independent experiments, each in duplicate).

From the analysis of the adsorption efficacy graphs (upper graphs of Figure 2.6), we can observe that when the lower protein concentration was used (100 µg/mL), differences among proteins or among particles do not exist. The differences become evident for the two higher protein concentrations. The myoglobin is the protein that is better adsorbed to the different types of NPs, whereas lysozyme is the one that is worse adsorbed.

To better understand these differences it is important to define the isoelectric point (pI), which is the pH at which a particular molecule carries no net electrical charge or, in other terms, is electrically neutral in the statistical mean (Salgin, S., Salgin, U. and Bahadir, S., 2012). At a pH below the pI, proteins will carry a net positive charge and, on the contrary, at a pH above the pI, they will carry a net negative charge. So, proteins with different pI will, consequently, be adsorved differently according to the pH of the solution, especially if the dominant interaction between particles and protein is an electrostatic interaction.

We can see from the analysis of the graphs that, for BSA (pI = 4.7), the PCL/CHI NPs are the ones that adsorbs it better. This can be explained because in water (pH ~ 5-6) BSA will acquire a negative charge that is likely to interact with the chitosan-positive residues exposed at the surface of the particles, resulting in a better efficacy of adsorption (Jesus, S. *et al.*, 2017). However, for the other proteins, myoglobin (pI = 7.1) and lysozyme (pI = 11.35), which were positively charged during the assay, hydrophobic interactions with particles maybe the dominant force since all the particles have hydrophobic polymers in its constitution. It should also be mentioned that at 100 µg/mL the AE (%) is 100 % in almost all cases and, therefore, this assay condition may be the better one to adopt in future assays, such as in uptake studies.

Furthermore, when analyzing the lower graphs of Figure 2.6, depicting adsorption capacity, we can see, in general, that the AC (%) increases when using 300 µg/mL of proteins, when comparing with the AC (%) at 100 µg/mL, whereas it remains the same when comparing with the AC (%) at 500 µg/mL. This fact indicates that the maximum capacity of the NP is achieved or, in other words, the quantity of the protein that is adsorved to the NP achieved the maximum value that is possible for the NP, so there is no advantage in using higher protein concentrations.

From these results, we can conclude that the different NPs are promising protein delivery systems, each of them being able to adsorb different types of proteins with different effectiveness.

Chapter 3 – Evaluation of the immunotoxicological profile of the different polymeric nanoparticles

Adapted from: DA SILVA, J., S. JESUS, N. BERNARDI, *et al.* Poly(D,L-Lactic Acid) Nanoparticle Size Reduction Increases Its Immunotoxicity. **Frontiers in Bioengineering and Biotechnology**, 2019, 7. DOI: 10.3389/fbioe.2019.00137.

3.1 Materials and Methods

3.1.1 *In vitro* studies using Whole Blood

3.1.1.1 Hemolysis Assay

Hemolysis assay was performed according to published protocols with minor modifications (Pattani, A. *et al.*, 2009, Villiers, C. *et al.*, 2009). Whole blood was collected from healthy donors after formal acceptance with a written informed consent and stabilized with lithium heparin as anticoagulant. Blood was diluted with phosphate-buffered saline (PBS) to adjust total blood hemoglobin (TBH) concentration to 10 mg/mL ± 2 mg/mL (TBHd). A volume of 100 µL of NPs suspensions, PBS (negative control) or Triton-X-100 (positive control) were added to 700 µL PBS in different tubes. Then, 100 µL of TBHd was added to each tube, followed by incubation at 37 °C for 3 h ± 15 min and every 30 min the samples were shaken. NPs were also incubated with PBS without blood to evaluate the possible NP interference. After the incubation time, the tubes were centrifuged at 800 g for 15 min. 100 µL of each supernatant and 100 µL cyanmethemoglobin (CMH) reagent were added to a 96-well plate. The CMH reagent was prepared by mixing 1000 mL Drabkin's reagent and 0.5 mL of 30 % Brij 35 solution (Sigma-Aldrich, St. Louis, MO, USA). The 96-well plate was left shaken during 2 to 3 min and the absorbance (OD) at 540 nm was measured using a microplate reader. Finally, the percentage of hemolysis was calculated by equation 4:

$$Hemolysis\ (\%) = \frac{(OD\ sample\ (540\ nm) - OD\ PBS\ (540\ nm))}{(OD\ TBHd\ (540\ nm) - OD\ PBS\ (540\ nm))} x\ 100 \qquad \text{(eq. 4)}$$

3.1.2 *In vitro* studies using Human Peripheral Blood Mononuclear Cells (PBMCs)

3.1.2.1 Isolation of mononuclear cells from human peripheral blood by density gradient

Buffy coats obtained from healthy donors (heparinized syringes) were kindly given by IPST, IP (Coimbra, PT). PMBCs were isolated on a density gradient with Lymphoprep (Axis-Shield, Dundee, Scotland) according to the provider's guidance protocol and as published by our group (Jesus, S. *et al.*, 2017), with minor modifications. Briefly, in a tube of 50 mL, the blood sample (1:5) was diluted in 0.9 % saline solution, homogenizing by inverting the falcon (6 mL blood: serum up to 30 mL). In new falcon tubes of 15 mL, with a Pasteur pipette, 2.5 mL of Lymphoprep were added (previously placed at room temperature (RT)) to each of them.

Then, 7.5 mL of the diluted sample were pipetted carefully onto the Lymphoprep, forming a layer thereon, without mixing. (For best addition, the tip of the pipette should be placed against the wall of the tube and let the sample be carefully poured). The samples were centrifuged for 20 min at 1190 g at 20 °C and a ring of mononuclear cells formed between the plasma / diluent liquid and the separation liquid.

After that, the liquid from the upper area was aspirated and the ring of mononuclear cells (white membrane - platelets, monocytes and lymphocytes) that exists at the interface between the plasma and Lymphoprep, especially at the periphery of the tube was carefully removed, in circular movements, and each 2 rings were placed in a new falcon tube of 15 mL. The collected suspension (every 2 rings) was diluted in PBS (pH 7.4) preheated to 37 °C up to 12 mL and tubes were homogenized by inverting and centrifuged for 10 min at 487 g at 20 °C. Finally, the supernatant was discarded by inverting the tube and the wash step was repeated 3 more times depending on the turbidity of the supernatant (corresponds to the elimination of platelets). After the last wash, the supernatant was discarded and the cells were resuspended in about 6 mL of Roswell Park Memorial Institute medium (RPMI), with 10 % heat inactivated fetal bovine serum (FBS), supplemented with 2 mM L-glutamine, 1 % penicillin/streptomycin and 20 mM HEPES.

3.1.2.2 Cell viability assays

NPs cytotoxicity was evaluated on human PBMCs using 3-(4,5-dimethylthiazol-2-yl)-2,5-diphenyltetrazolium bromide (MTT) assay. Cells were plated in a 96-well plate at a density of 5 x 10^5 monocytes/well for 24 h. Serial dilutions of NPs and controls were incubated with the cells for 22 h, at 37 °C and 5 % CO_2. After this period, 20 µL of MTT solution at 5 mg/mL (previously prepared in PBS at pH=7.4 and filtered to remove any precipitate with filters of 0.22 µm) were added to each well followed by additional 4 h incubation. To ensure dissolution of the formazan crystals, cell culture plates were centrifuged (800 g, 25 min, 20 °C) and the culture medium was replaced by dimethyl sulfoxide (DMSO) and the OD of the resultant colored solution was measured at 540 nm and 630 nm. Cell viability (%) was calculated by equation 5:

$$Cell\ viability\ (\%) = \frac{(OD\ sample\ (540\ nm) - OD\ sample\ (630\ nm))}{(OD\ control\ (540\ nm) - OD\ control\ (630\ nm))} \times 100 \qquad \text{(eq. 5)}$$

The inhibitory concentration for 50 % of cell viability (IC_{50}) was calculated by plotting the log concentration of the NPs versus inhibition percentage of cell viability and extrapolating the value from a non-linear regression using Prism 6.0 (GraphPad Software, San Diego, CA, USA).

Cytotoxicity results obtained with MTT assay were confirmed with propidium iodide (PI) assay. Briefly, cells incubated during 22 h with 4 nanoparticle concentrations previously used in MTT assay were centrifuged (800 g, 25 min, 20 °C), resuspended in PBS and collected for analysis in a BD FACSCalibur Flow Cytometer (BD Biosciences, Bedford, MA, USA) using PI solution (0.5 µg/mL).

3.1.2.3 Quantification of cytokines

The stimulation of cytokines production (tumor necrosis factor-α (TNF-α) and interleukin 6 (IL-6)) was evaluated by enzyme-linked immunosorbent assay (ELISA). For that, the cells were plated in a 96-well plate at a density of $2.5x10^5$ cell/well and 125 µL of the samples (different NPs under test and their respective vehicle controls (VCs)), prepared endotoxin-free, were added thereon at a final concentration in the well of 100 µg/mL. Concanavalin A (ConA) (5 µg/mL) and lipopolysaccharide (LPS) (2 ng/mL) were used as positive controls. After 22 h of incubation at 37 °C and 5 % CO_2, the plate was centrifuged for 25 min at 800 g and 220 µL of the supernatants were carefully aspirated without disturbing the cells at the bottom of the well and stored at -80 °C until cytokines analysis.

A ELISA technique was used, in order to measure cytokines production according to kit manufacturer's instructions Human TNF- α and IL-6 Standard ABTS ELISA Development Kit from PeproTech (Rocky Hill, NJ, USA). In short, 100 µL of capture antibody at a concentration of 1.0 µg/mL were added to a high binding 96-well plate and left incubating overnight at RT. Then, the plate was washed 4 times with wash buffer and incubated for at least 1 h at RT with block buffer. The plate was washed again 4 times and serial dilutions from 2000 pg/mL to zero of TNF-α or from 1500 pg/mL to zero of IL-6, as well as 100 µL of each sample were added to each well in triplicate. The plate was left incubating for more 2 h at RT. Each sample represented a pool of one condition done in triplicate in one day. Once again, the plate was washed 4 times and 100 µL of detection antibody at a concentration of 0.50 µg/mL were added to each well and left incubating for 2 h at RT. After 4 more washes, 100 µL of avidin-HRP conjugate were added and left incubating for 30 min at RT. The plate was washed 4 last times and 100 µL of substrate solution were added to each well and left incubating at RT for color development. Finally, an absorbance plate reader was used to monitor color development at 405 nm with

wavelength correction set at 650 nm and concentration of released cytokines were extrapolated from absorbance values, using the calibration curves.

Cell viability assay was also performed under this assay conditions, in order to evaluate if the concentrations tested had the ability to induce toxicity. For that, resazurin cell viability assay was performed, which is another colorimetric reagent, also known as Alamar Blue dye, that is used as an oxidation-reduction indicator in cell viability assays. After collecting the supernatants of the 24 h incubation, the cells were incubated with 100 µL of 10 % (v/v) Alamar Blue dye in complete DMEM medium, prepared from a 0.1 mg/mL stock solution of Alamar Blue, for 72 h at 37 °C and the OD of the resultant colored solution was measured at 570 nm and 600 nm. Cell viability (%) was calculated by equation 6:

$$Cell\ viability\ (\%) = \frac{(OD\ sample\ (570\ nm) - OD\ sample\ (600\ nm))}{(OD\ control\ (570\ nm) - OD\ control\ (600\ nm))} \times 100 \qquad \text{(eq. 6)}$$

Furthermore, endotoxin contamination of the samples used in ELISA (diluted in RPMI medium) was also assessed using the Pyrochrome® Limulus Amoebocyte Lysate (LAL) endpoint assay (Associates of Cape Cod, Inc., East Falmouth, MA, USA) according to the kit manufacturer's instructions. Briefly, 50 µL of Pyrochrome® were rapidly added to all the samples (pyrogen-free water, endotoxin standards for calibration curve, and the different samples to be tested) at a ratio of 1:1, mixed from 5 to 30 seconds and incubated for 28 min. After incubation, the reaction was stopped by adding 25 µL of 50 % acetic acid and the OD was measured at 405 nm. The quantification of LPS was extrapolated from the standard curve, constructed by plotting optical density readings against standard endotoxin concentrations.

3.1.2.4 Protein uptake studies

To evaluate the capacity of the different NPs of this study as therapeutic protein delivery systems, BSA was adsorbed to the different NPs and, posteriorly, cellular uptake studies were performed. For that, the different NPs were incubated at a concentration of 70 µg/mL with BSA (100 µg/mL), labeled with fluorescein isothiocyanate (FITC) from Santa Cruz Biotechnology (Santa Cruz, CA, USA). PBMCs seeded in a 48-well plate at a density of 1.25×10^6 cells/well were incubated for 4 h with NPs-BSA-FITC. Free BSA-FITC was also incubated in the same conditions, to serve as a comparison term. After the 4 h incubation, the cells were washed with 100 µL of PBS, detached with 100 µL of 5 x trypsin and suspended in 100 µL of supplemented RPMI. Then, the cells were centrifuged for 20 min at 487 g at 20 °C and resuspended in 200 µL of ice-cold PBS for further cytometry analysis.

Accordingly, for cytometry analysis, cells with the different samples were split in two different analysis tubes: one with 1 µL of 50 µg/mL PI solution and the other with 100 µL of 0.4 % trypan blue solution added prior BD FACSCalibur Flow Cytometer (BD Biosciences, San Jose, CA, USA) analysis. Finally, the fluorescence data for a population of 20000 lymphocytes was collected and the results processed by CellQuestModfit LT software.

For cell viability analysis, the same protocol described above was performed and 25 µL of MTT solution at 5 mg/mL were added to each well, followed by additional 4 h incubation. Then, plates were centrifuged for 25 min at 800 g at 20 °C, posteriorly, the culture medium was replaced by DMSO and, lastly, the OD of the resultant colored solution was measured at 540 nm and 630 nm. Cell viability (%) was calculated as explained above.

Furthermore, for confocal microscopy analysis, cells were seeded on glass coverslips in 24-well plates at a density of $2.5x10^6$ cells/well and incubated overnight prior assay, performed as described above. After particles incubation, cells were washed three times with PBS and fixed with 4 % PFA in PBS for 15 min at 37 °C. The nucleus and cell membrane were labeled using Image-iTTM LIVE Plasma Membrane and Nuclear Labeling Kit (Hoechst 33342 and Alexa Fluor® 594; Life Technologies Corporation, Paisley, UK), respectively. After labeling, cells were washed twice with PBS and the coverslips mounted in microscope slides with DAKO mounting medium. Samples were examined under an inverted laser scanning confocal microscope (LSCM) (Zeiss LSM 510 META, Carl Zeiss, Oberkochen, Germany).

Cell viability assay was also performed under this assay conditions, in order to evaluate if the concentrations used were inducing any toxicity. For that, after the 4 h of incubation with the different samples, the cell viability was assessed through the MTT assay, as previously described.

3.1.3 *In vitro* studies with RAW 264.7 Macrophage Cell Line

3.1.3.1 Cell Culture

RAW 264.7 (ATCC® TIB-71™) were acquired to ATCC (Manassas, VA, USA), cultured in Dulbecco's Modified Eagle Medium (DMEM), supplemented with 10 % heat inactivated FBS, 1 % Penicillin/Streptomycin, 10 mM HEPES and 3.7 g/L Sodium Bicarbonate, and used until passage 18. Briefly, the old medium was removed of the flask by aspiration and 12 mL of new DMEM medium (previously heated up to 37 °C) were added. Then, the adhered cells were scraped with a scraper and gently stirred manually. From the flask, a certain volume of the cell suspension was removed depending on the dilution factor chosen (1:3 to 1:8 is

recommended (ATCC)) and added to a new flask (75 cm^3) with 20 mL of fresh DMEM medium and gently stirred manually. Finally, the cells were incubated at 37 °C and 5 % CO_2 until they were ~80 % confluent (48 h to 120 h).

3.1.3.2 Cell viability assays

NPs toxicity in RAW 264.7 was assessed as described previously for PBMCs with some modifications. Briefly, for MTT assay, macrophages were plated at a concentration of 2 x 10^4 cells/well and the incubation with MTT solution was performed for 90 min. Then, the medium was removed by aspiration and the formazan crystals were dissolved with 100 µL of DMSO. Finally, the absorbance was read at 540 and 630 nm reference filter.
For PI assay, the cells were collected using a dissociation medium (PBS-EDTA 5 mM) followed by centrifugation (250 g, 10 min, 20 °C) to replace the medium with PBS.

3.1.3.3 Reactive Oxygen Species Production Assay

Reactive oxygen species (ROS) production was assessed using the dichlorofluorescein diacetate probe (DCFH-DA) (Thermo Fisher Scientific Inc., Waltham, MA, USA). The RAW 264.7 cells were incubated in a black 96-well plate for 24 h at 37 °C and 5 % CO_2, at density of 0.5 x 10^5 cells/well. After that period, serial dilutions of NPs were incubated with the cells for 22 h at 37 °C and 5 % CO_2, to evaluate ROS stimulation, using LPS as a positive control at 1 µg/mL.
After 22 h, cell culture medium was replaced by DCFH-DA at 50 µM in serum-free DMEM and the cells were incubated for another 2 h at 37 °C and 5 % CO_2. The resulting fluorescence was read at 485/20 nm and 528/20 nm (excitation/emission wavelengths).
To calculate the ROS production, equation 7 was applied:

$$ROS\ production\ (mean\ fluorescence\ increase) = \frac{Fluorescence_{SAMPLE}}{Fluorescence_{NEGATIVE\ CONTROL}} \quad \text{(eq. 7)}$$

3.1.3.4 Nitric Oxide Production Assay

Nitric oxide (NO) production by RAW 264.7 was evaluated based on nitrite quantification using the Griess reagent. RAW 264.7 cells were incubated in a 48-well plate at a density of 2.25 x10^5 cells/well for 24 h at 37 °C and 5 % CO_2. After that period, cell culture medium was replaced by serial dilutions of NPs diluted in cell culture medium without phenol red.

LPS was used as a positive control at 1 µg/mL. To test if the NPs were able to inhibit LPS stimulated NO production, the same NP concentrations were incubated together with LPS at 1 µg/mL.

Cell supernatants were collected 22 h after incubation, and 100 µL of each test sample was plated in a 96-well plate and combined with an equal volume of Griess reagent. A calibration curve performed with sodium nitrite (from 0 µg/mL to 80 µg/mL) was also plated in duplicate. Finally, the 96-well plate was kept at RT for 10 min in the dark and, subsequently, the optical density of the samples was measured at 550 nm and NO quantification was extrapolated from the calibration curve.

To calculate the inhibition of NO production upon stimulation with LPS equation 8 was applied:

$$Inhibition\ of\ NO\ production\ (\%) = \frac{NO(\mu g/mL)_{\ SAMPLE}}{NO\ (\mu g/mL)_{\ POSITIVE\ CONTROL}} \times 100 \qquad \text{(eq. 8)}$$

3.1.4 Statistical analysis

Data were analyzed using GraphPad Prim 6 (GraphPad Software, Inc., La Jolla, CA, USA), in which significant differences were obtained from one-way ANOVA, or Wilcoxon matched-pairs signed rank test in case of ELISA, and values were considered statistically different when $p < 0.05$. *In vitro* data were expressed as means ± standard error of the mean (SEM).

3.2 Results and Discussion

3.2.1 All developed polyester NPs are hemocompatible

Hemolysis is the breakdown of red blood cells with subsequent release of intracellular contents. *In vivo*, this can lead to anemia or other pathological conditions (Dobrovolskaia, M.A. *et al.*, 2008). It is important to assess the NP effect on these blood elements not only when the intravenous route of administration is considered but also when addressing other administration routes, in order to establish their hemocompatibility (Dobrovolskaia, M.A. *et al.*, 2008). For that reason, NP hemocompatibility was assessed in human whole blood and hemolytic values were considered above 5%, as recommended by American Society for Testing and Materials International (ASTM, 2013). Results are presented in Figure 3.1.

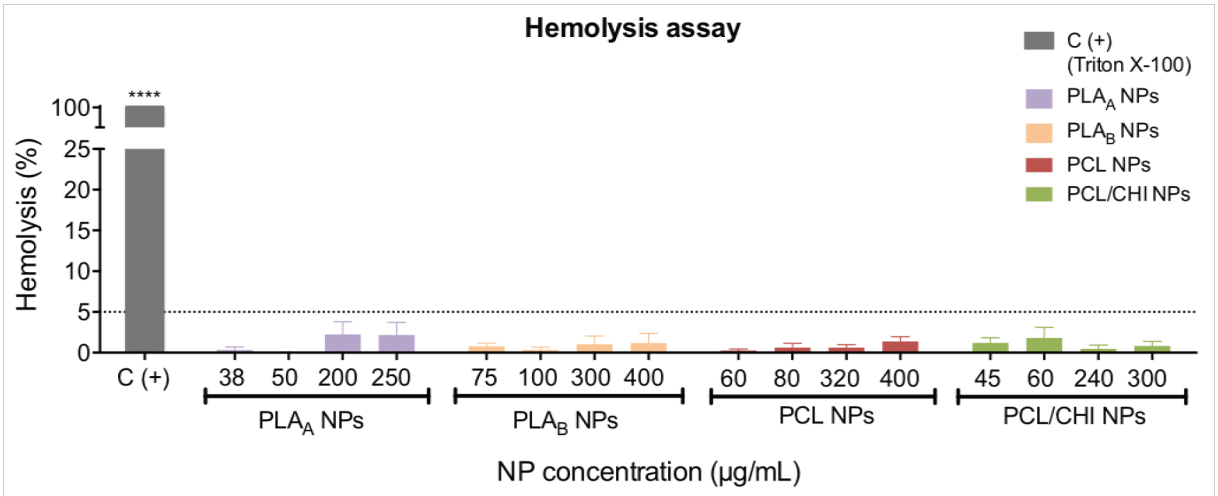

Figure 3. 1 – Hemolytic activity of NPs in human blood after 3 h of incubation at 37° C. Triton X-100 was used as a positive control. Hemolytic values were considered above 5 %, as recommended by American Society for Testing and Materials International (ASTM, 2013). Data are presented as mean ± SEM, n≥3 (three or more independent experiments, each in duplicate).

The results (Figure 3.1) showed that all NPs had a good hemocompatibility profile. In fact, hemolysis values below 5 % were observed for all NPs tested under the concentration range tested (38 µg/mL to 250 µg/mL for PLA$_A$ NPs; 75 µg/mL to 400 µg/mL for PLA$_B$ NPs; 60 µg/mL to 400 µg/mL for PCL NPs; 45 µg/mL to 300 µg/mL for PCL/CHI NPs).

According to our results, both PLA NPs did not present hemolytic activity in concentrations up to 250 µg/mL and 400 µg/mL for PLA$_A$ and PLA$_B$ NPs, respectively. To note that these are very high concentrations, far from the reality of *in vivo* administrations. In fact, apart from the fact that the experiment is performed with diluted blood (> 10 times diluted), 250 µg/mL would correspond to a intravenously injected human dose of 1400 mg of NP and 400 µg/mL to a dose of 2240 mg (in a 70 kg person, with 5.6 L of blood (Dobrovolskaia, M.A. and

McNeil, S.E., 2013)). Results confirm therefore the hemocompatibility of PLA NPs, accordant with Altmeyer and co-workers, who described that no erythrocyte damage was caused by blank PLA NPs produced by an emulsion/solvent evaporation method with polyvinyl alcohol (PVA) (Altmeyer, C. *et al.*, 2016).

Moreover, results also showed that both PCL and PCL/CHI NPs did not present hemolytic activity in concentrations up to 400 µg/mL and 300 µg/mL, respectively. These results confirmed the hemocompatibility of the different polymeric NPs and can be related to some previously published papers studying other polymeric NPs. In fact, the results are in agreement with Sarangapani and co-workers, since they found no significant hemolysis caused by CHI NPs in concentrations between 50 µg/mL and 300 µg/mL (Sarangapani, S. *et al.*, 2018). On its turn, according to Shelma and Sharma, CHI NPs were slightly hemolytic (~7 %) in the concentration of 2000 µg/mL (Shelma, R. and Sharma, C.P., 2011), which is a much higher concentration than the concentration used in this assay, and is important to highlight here again that they were far from the reality of *in vivo* administrations (Dobrovolskaia, M.A. and McNeil, S.E., 2013). Subsequently, this study reinforced the importance of performing a case-by-case evaluation of NP immunotoxicological profile.

3.2.2 None of the developed polyester NPs induce cytotoxicity in PBMCs

The colorimetric MTT assay for measuring cell metabolic activity is based on the cellular conversion of a tetrazolium salt (MTT) into an insoluble formazan, that can be dissolved in DMSO generating a purple signal (Altmeyer, C. *et al.*, 2016). Therefore, through an indirect way, MTT assay was used to evaluate the cytotoxicity of different NPs after 24 h incubation with PBMCs. Results are presented in Figure 3.2.

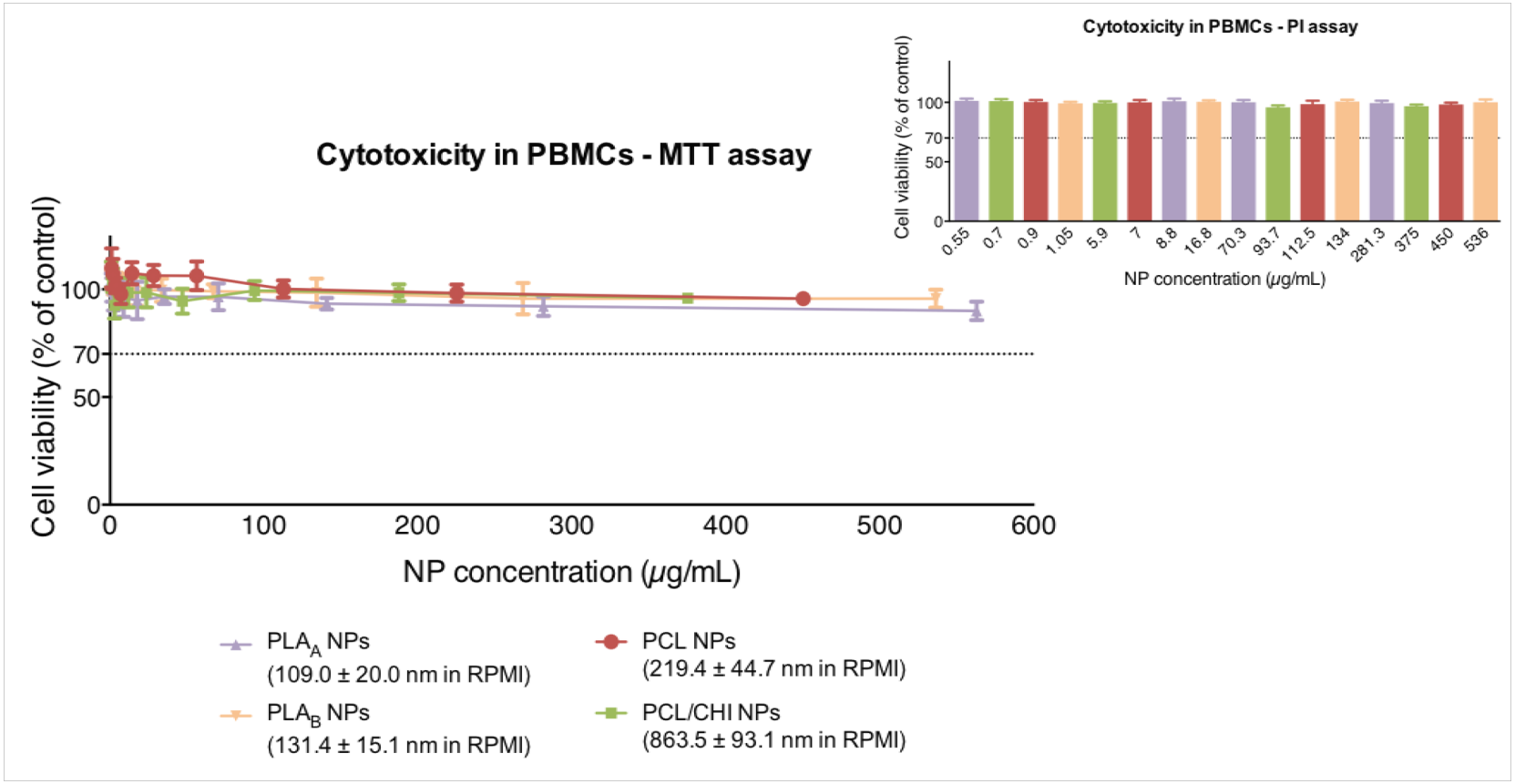

Figure 3. 2 – Cytotoxicity assays (MTT and PI), performed in PBMCs after 24 h of incubation with different NPs. Data are presented as mean ± SEM, n≥4 (four or more independent experiments, each in triplicate).

Results presented in Figure 3.2 showed that none of the NPs of this study induced cytotoxicity in PBMCs, since the incubation with each one of them resulted in cell viabilities above 70 % under the concentration range tested (0.55 µg/mL to 562.5 µg/mL for PLA_A NPs; 1.05 µg/mL to 536 µg/mL for PLA_B NPs; 0.9 µg/mL to 450 µg/mL for PCL NPs and 0.7 µg/mL to 375 µg/mL for PCL/CHI NPs). For PLA NPs, the similarity in the cytotoxicity profile in this primary culture could be explained by the similar mean diameter and zeta potential of the NPs when dispersed in RPMI medium, as demonstrated in the NP characterization in the different experiment conditions. In fact, the differences in size previously seen in pyrogen-free water were masked in RPMI.

When analyzing the results obtained for PCL and PCL/CHI NPs, we can also observe a similarity in the cytotoxicity profile in this primary culture. However, the same explanation as the one used for PLA NPs could not be used here. In fact, PCL and PCL/CHI NPs did not present a similar mean diameter and zeta potential. Data from the NP characterization in the experiment conditions revealed that PCL NPs presented a similar mean diameter in RPMI as in pyrogen-free water, while PCL/CHI NPs presented a larger mean diameter in RPMI when compared with the one obtained in pyrogen-free water, resultant from a higher heterogeneity of the NP population.

In order to avoid possible excessive assumption regarding cytotoxicity when using only a metabolic assay, these results were confirmed with PI assay, which evaluates the integrity of the cell membrane. Results were similar to the ones obtained with MTT (Figure 3.2).

When comparing our results to other results from the literature, Jesus and co-workers observed a cell viability decrease of almost 50 % in PBMCs with PCL/CHI NPs at a concentration of 40 µg/mL (Jesus, S. *et al.*, 2017). This fact is contradictory with our results, since even with much higher NP concentration, we never achieved decreases in cell viability in PBMCs. However, it is to emphasize that they used a lower concentration of cells for their experiment ($1x10^6$ cells/mL) than the one we used ($5x10^6$ monocytes/mL), what could be an explanation for such differences. In fact, the absence of cytotoxicity in PBMCs was verified for the conditions used in the assay, i.e. the number of cells, the incubation time and the concentrations of NPs. In our assay, we used 5×10^5 monocytes/well ($5x10^6$ monocytes/mL) but other cells were present in the assay, namely lymphocytes. The total number of cells used was 7.5×10^6 cells/well. The present conditions were different from what was possible to found in the literature and, therefore, could explain the differences observed.

Consequently, we can emphasize the importance of understanding correctly the differences observed because they can be related with the methodology used. In fact, a multitude of variables such as different NPs, produced with different polymers, different surfactants, and different assay conditions, can lead to different results when evaluating cytotoxicity.

3.2.3 Endotoxin-free NPs do not stimulate the production of cytokines by PBMCs

Cytokines are important signaling molecules involved in the acute phase of immune response to injury and infection (Arango Duque, G. and Descoteaux, A., 2014, Mohan, M.L., Vasudevan, N.T. and Naga Prasad, S.V., 2017). After pathogens recognition, monocytes and macrophages, the essential components of the innate immune system, release proinflammatory cytokines, including interleukin 1 (IL-1), IL-6 and tumor necrosis factor alpha (TNF-α) (Boshtam, M. *et al.*, 2017, Mohan, M.L., Vasudevan, N.T. and Naga Prasad, S.V., 2017, Parihar, A., Eubank, T.D. and Doseff, A.I., 2010). When in contact with the components of the immune system, NPs can be seen as invaders and, consequently, induce the production of proinflammatory molecules. Therefore, in this work the production of two cytokines, TNF-α and IL-6, were evaluated by ELISA in the supernatants of PBMCs, after incubation with NPs. For that, the different endotoxin-free NPs under test were incubated at 100 μg/mL for 24 h with PBMCs.

One of the first proinflammatory cytokines released from monocytes and macrophages in response to pathogens is TNF-α, which is involved in the regulation of apoptosis, survival and immune responses (Arango Duque, G. and Descoteaux, A., 2014, Cai, X. *et al.*, 2017, Young, S.H. *et al.*, 2001). Thus, the quantification of its production is fundamental to evaluate the influence in inflammatory responses mediated by the different NPs under test. Results are presented in Figure 3.3.

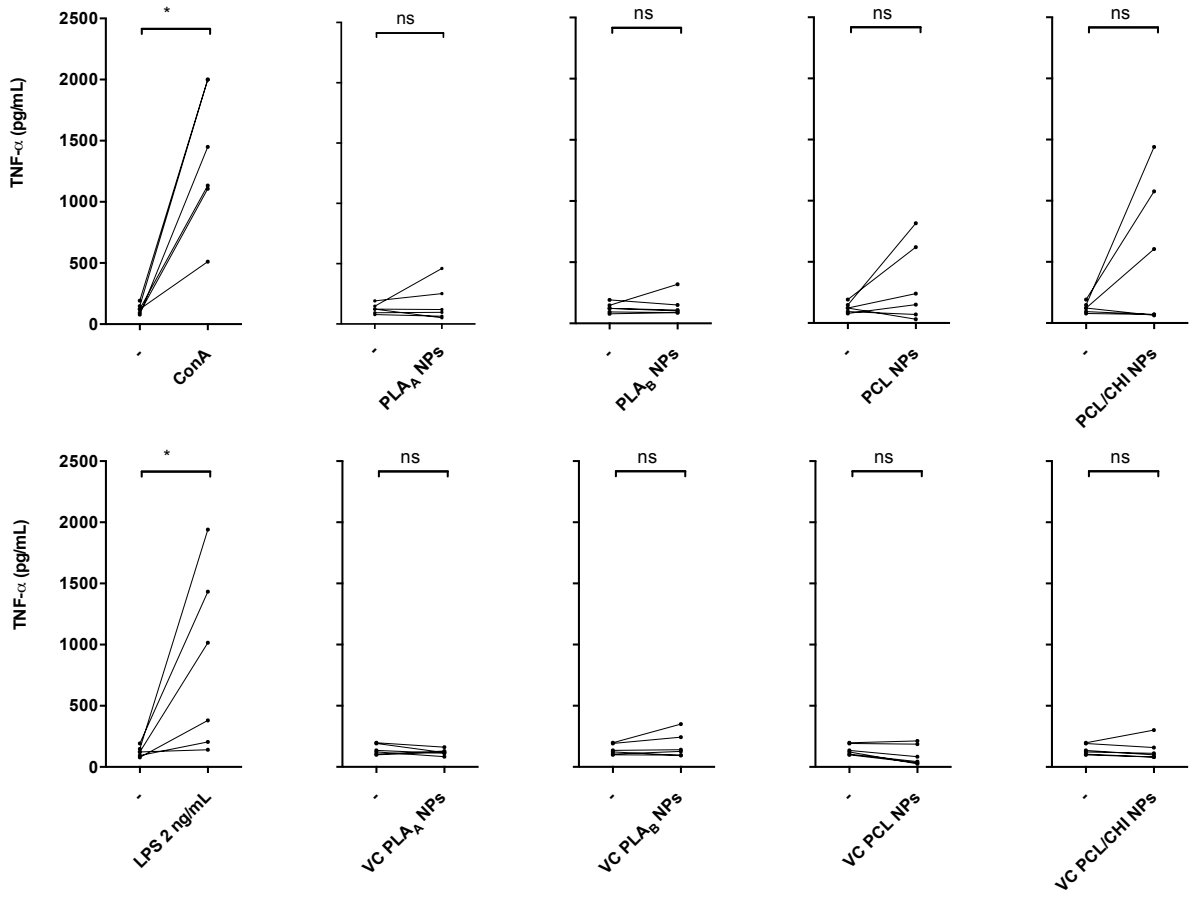

Figure 3. 3 – Effect of different NPs on TNF-α production in PBMCs. The concentration of TNF-α represented in pg/mL. This cytokine was measured using commercially available ELISA kits. ConA 5 µg/mL and LPS 2 ng/mL were used as positive controls. Supernatants were harvested after 24 h of incubation with the formulations. Results represent the mean ± SEM, n=6 (experiment performed in PBMCs isolated from 6 different healthy donors).

In the graphs from figure X we can observe the different conditions under which the TNF-α production was tested, and in each graph each line represents a different donor before and after the stimulation. ConA and LPS were used as positive controls and it is visible the increase in the TNF- α production upon stimulation. On the other hand, none of the PLA NPs in this study stimulate significantly TNF-α production. The same conclusion can be drawn to the respective solvent controls (VC). However, with PCL-based NPs, a tendency to show high values with some donors was observed (Figure 3.3). For instance, with PCL/CHI NPs, PBMCs from 3 of the 6 donors tested produced high levels of TNF-α, similar to LPS control. To confirm these results more donors must be tested.

According to literature, at a concentration of 300 µg/mL, PLA and PCL NPs lead to a 1.5 to 2-fold increase in TNF- α release. However, Singh and Ramarao used a three times higher NP concentration in their assay, what could explain the induction of TNF-α release. Moreover, they did not refer if the NPs used were endotoxin-free, which could be an

additional explanation of these contradictory results. Wang and co-workers also analyzed the induction of TNF-α release with CHI stabilized PLLA and PDLA NPs and they observed that the presence of the stabilizer chitosan in the NP structure seemed to slightly increase the production of the cytokine TNF-α, but without significant differences from negative control, which is concordant with our results (Wang, Q. *et al.*, 2014). Similarly, Grabowski and co-workers also demonstrated that CHI/poly(lactic-co-glycolic acid) (PLGA) NPs (at 100 μg/mL) induced the production of TNF-α, still without hitting statistical difference (Grabowski, N. *et al.*, 2015, Grabowski, N. *et al.*, 2016).

Another important proinflammatory cytokine released from monocytes and macrophages in response to pathogens is IL-6, which is involved in processes ranging from immunity to tissue repair and metabolism (Arango Duque, G. and Descoteaux, A., 2014). Thus, the quantification of its production is also crucial to evaluate the influence in inflammatory responses mediated by the different NPs under test. Results are presented in Figure 3.4.

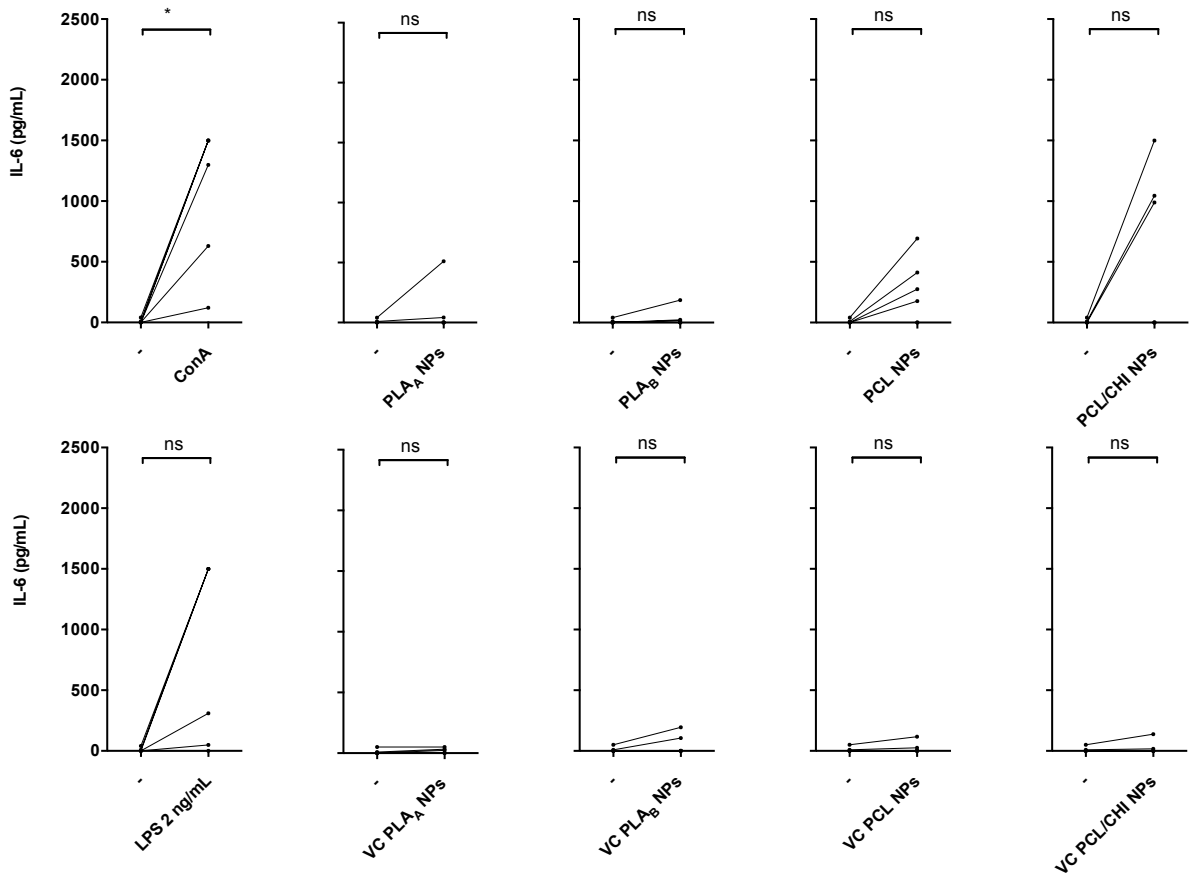

Figure 3. 4 – Effect of different NPs on IL-6 production in PBMCs. The concentration of cytokine IL-6 represented in pg/mL. This cytokine was measured using commercially available ELISA kits. ConA 5 µg/mL and LPS 2 ng/mL were used as positive controls. Supernatants were harvested after 24 h of incubation with the formulations. Results are the mean ± SEM, n=6 (experiment performed in PBMCs isolated from 6 different healthy donors).

Again, we used ConA and LPS as positive controls (Figure 3.4). It was observed a reasonable variation among donors, when stimulated with mitogens (positive controls). The LPS stimulation was found not to induce a statistically significant increase in IL-6 production. In fact, the PBMCs from one donor did not produce IL-6, influencing the statistics. Nevertheless, results from ConA were positive and therefore, no donor was excluded. Regarding NP results, although the statics treatment of the results indicated that none of the NPs of this study was able to stimulate IL-6 production significantly, the truth is that the cells of some donors showed a great stimulation, particularly with PCL- based NPs. On the other hand, IL-6 concentration found for cells treated with the solvent controls (VC) was similar to the negative control (unstimulated cells).

All in considered, the results are in agreement with the literature, since neither PLA NPs nor PCL NPs induce IL-6 release when tested at a concentration of 300 µg/mL (Singh, R.P. and Ramarao, P., 2013). Besides that, according to Grabowski and co-workers, the presence

of the stabilizer chitosan in the structure of PLGA NPs at a concentration of 100 µg/mL seems to slightly increase the production of IL-6, as we also demonstrated, however without significant differences (Grabowski, N. *et al.*, 2015, Grabowski, N. *et al.*, 2016). Correspondingly, Grabowski also related the importance of precise knowledge of NP composition, since differences in stabilizers may alter the NP toxicological profile (Grabowski, N. *et al.*, 2015).

To highlight, when working with primary cells one should be careful with the variability between donors. Indeed, as illustrated with this study, PBMCs from 6 different donors originated some discrepant results, even in the positive controls. Even so, all the results are meaningful, and to increase their robustness more donors would need to be tested.

Importantly, we also evaluated the cytotoxicity of the samples under these experimental conditions as the results could be biased if the concentrations used were inducing any toxicity. For that, after collecting the supernatants of the 24 h incubation, cell viability was assessed through the resazurin assay, which is another colorimetric reagent that is used as an oxidation-reduction indicator in cell viability assays, and none of the samples of ELISA presented cell viabilities below 70 % under these experimental conditions. Thus, none of the samples is affecting the reliability of the assay.

Furthermore, endotoxin contamination of the NP samples used to stimulate the cells (diluted in RPMI medium) was also assessed through the Pyrochrome® LAL assay, based on the amebocyte lysate method. In the presence of endotoxin, the proenzyme Factor C, found in circulating ameboytes of the horseshoe crab *Limulus Polyphemus* is activated in a proteolytic cascade, resulting in the cleavage of a colorless artificial peptide substrate present in Pyrochrome® LAL. This proteolytic cleavage leads to the liberation of para-nitroaniline (pNA), which is yellow and could be measured by reading absorbance at 405 nm. Results are presented in Figure 3.5.

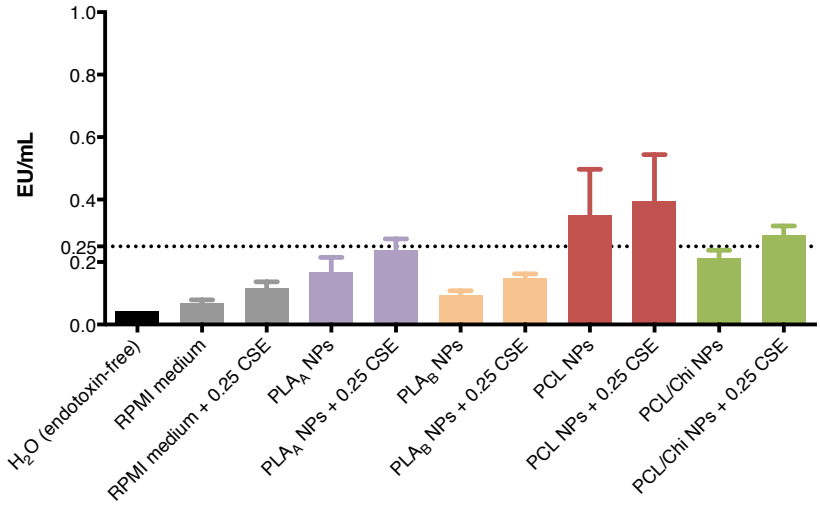

Figure 3. 5 – Pyrochrome® LAL assay with the samples used in PBMC stimulation for cytokine production (diluted in RPMI medium). Pyrogen-free water was used as negative control and the calibration curve was performed using the control standard endotoxin (CSE). Results were extrapolated from the calibration curve and are presented as the mean ± SEM, n=2 (two independent batches, each in duplicate).

When analyzing Figure 3.5, it is possible to acknowledge that pyrogen-free water (negative control), as expected, presented a very low amount of endotoxin contamination. Also, RPMI medium presented a slightly higher amount of endotoxin but still below 0.25 EU/mL threshold (dotted line), which is the limit for sterile injection water (European Pharmacopeia, 2016). Concerning the different NPs under test, both PLA NPs and PCL/CHI NPs presented a slightly higher amount of endotoxin but still below 0.25 EU/mL threshold, whereas PCL NPs presented a much higher amount of endotoxin with values above 0.25 EU/mL threshold. However, PCL NPs are not the ones that lead to highest increase in cytokine release, so it may not be related.

Nonetheless, the interferences with the assay (enhancement/inhibition) were tested as recommended by the kit manufacturer, by spiking the samples with a known amount of CSE (we selected 0.25 EU/mL) and analyzing the results. Results of the spiking are represented also in the graph. Despite there was an increase in all samples, the increase was not within the limit of 50 % to 200 % of 0.25 EU/mL (results were analyzed by subtracting the value of the sample from the value of the sample + CSE). With this we found that, probably the medium was interfering with the assay, and, consequently, the reliability of the assay was affected. Besides that, previous results from our laboratory group showed that que quantity of LPS used as positive control (2 ng/mL) in the cytokine production assay presented values above the calibration curve maximum tested (1 EU/mL). In fact, we can hypothesize that the

endotoxin contamination present in the samples had much lower potency than the positive control of LPS.

All in consideration, we cannot fully rely on these results and can conclude that cytokine production assays should also be repeated in the presence of polymyxin B to mitigate the effects of LPS if it is actually present in the samples, increasing the robustness of the assay.

3.2.4 All developed polyester NPs seem to increase BSA uptake, however without hitting statistical difference

In order to evaluate the ability of the different NPs of this study to be a protein delivery systems and so, to facilitate the entry of the protein into the cell, BSA-FITC was adsorbed to the different NPs and, posteriorly, cellular uptake studies were performed with PBMCs. The cells were analyzed by flow cytometry and results are presented in Figure 3.6.

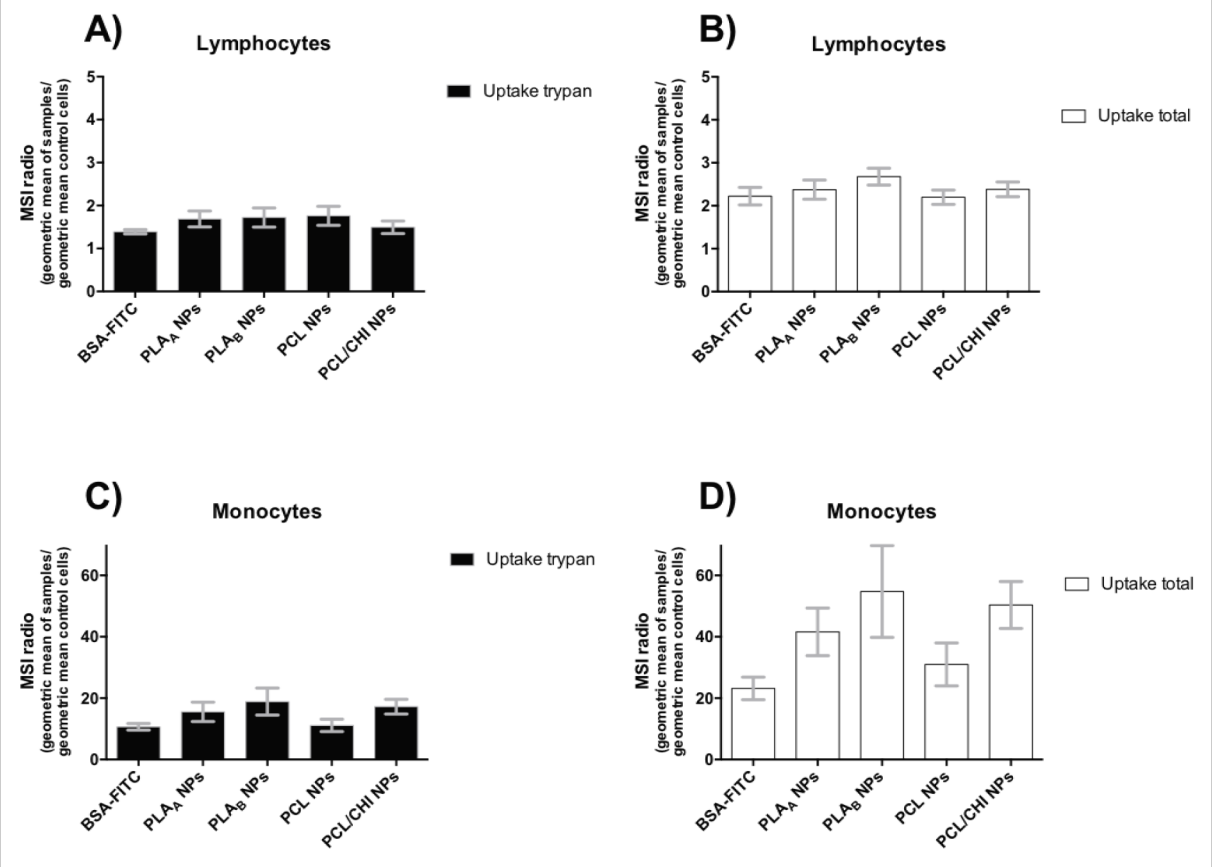

Figure 3. 6 – Flow cytometry analysis of PBMCs reflecting the results of the uptake studies with PBMCs after 4 h incubation with different BSA loaded NPs and BSA only (control). The results are expressed as mean fluorescence intensity (MFI) ratio between the geometric mean of the sample and the geometric mean of the background. A) Lymphocytes analyzed in the presence of trypan blue. B) Lymphocytes (internalized + cell surface interaction). C) Monocytes analyzed in the presence of trypan blue. D) Monocytes (internalized + cell surface interaction). Results are the mean ± SEM, n=3 (three independent experiments, each in duplicate).

When NPs reach the exterior membrane of a cell, they can interact with components of the plasma membrane or extracellular matrix, enter the cell and deliver their contents (Behzadi, S. *et al.*, 2017). So, when analyzing Figure 3.6A and 3.6B, we can see that none of the NPs of the study lead to an increase on the uptake of BSA-FITC in lymphocytes when comparing with free BSA-FITC. However, in monocytes, the presence of the NPs seems to increase the uptake of BSA-FITC, specially with PLA_B NPs and PCL/CHI NPs, since they more than duplicate the uptake of BSA-FITC. Nonetheless, these results did not have statistical difference in comparison to free BSA-FITC as the disparity in results obtained with different donors was high (Figure 3.6C and 3.6D).

Importantly, we also evaluated the cytotoxicity of the samples under these experimental conditions. For that, after the 4 h of incubation with the different samples, the cell viability was assessed through the MTT assay. None of the BSA-FITC adsorbed NPs under test showed to induce a decrease of cell viability above 70 %.

In order to illustrate the particle internalization into PBMCs, images from confocal microscopy were obtained. The representative images are presented in Figure 3.7.

A) Free BSA

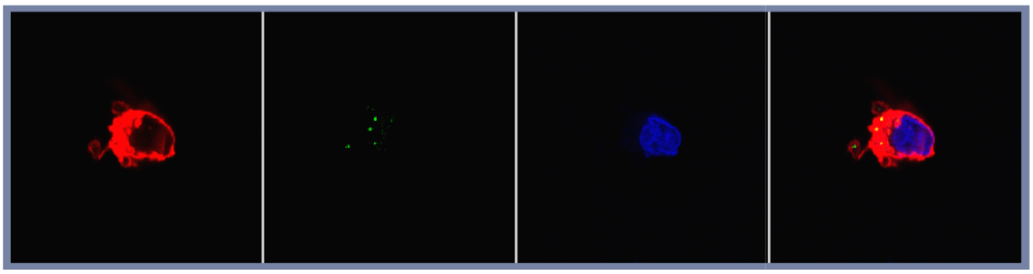

B) PLA_A NPs

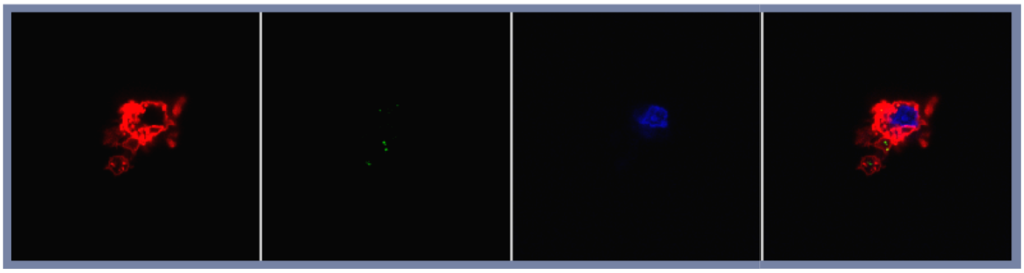

C) PLA_B NPs

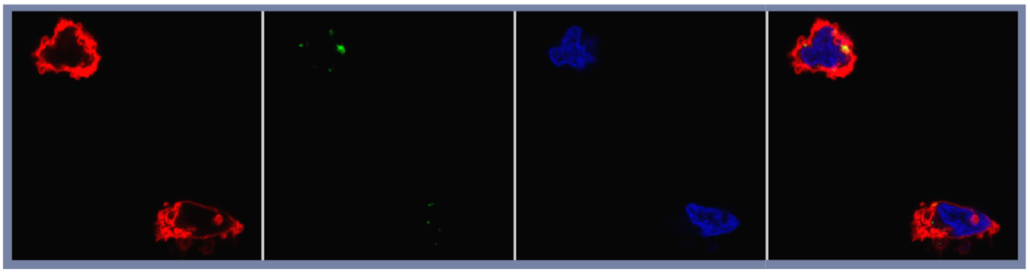

D) PCL NPs

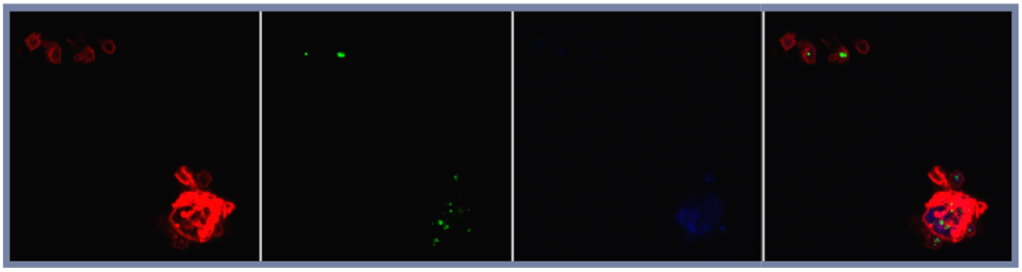

E) PCL/CHI NPs

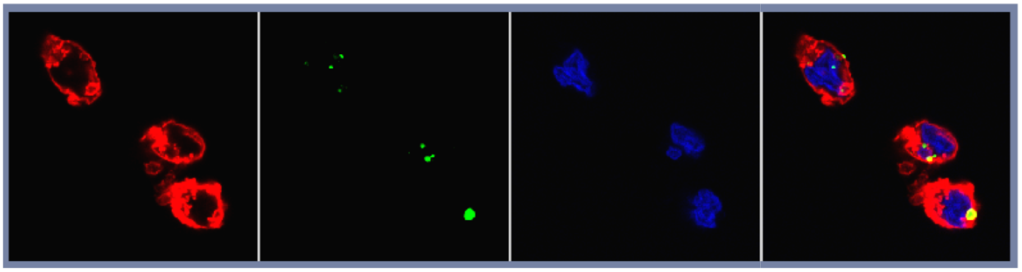

Figure 3. 7 – Confocal microscopy images of PBMCs after 4 h of incubation with FITC-BSA loaded NPs and free BSA. A) Free BSA. B) FITC-BSA loaded PLA_A NPs. C) FITC-BSA loaded PLA_B NPs. D) FITC-BSA loaded PCL NPs. E) FITC-BSA loaded PCL/CHI NPs.

The images from the confocal microscopy confirmed that free BSA are able to be internalized by PBMCs. The BSA adsorbed on particle surface were also able to be

internalized into cells. Concerning PLA_A NPs, we expected to observe an increase of BSA-FITC uptake in monocytes when compared with free BSA-FITC as observed in flow cytometry analysis, however this fact was not observable in confocal microscopy images (Figure 3.7B). Nevertheless, we can see that PLA_B NPs (Figure 3.7C) lead to a higher uptake of BSA-FITC in monocytes when compared with PLA_A NPs (Figure 3.7B), especially on cell surfaces which was also observed in the flow cytometry assay. Apparently, PCL NPs also lead to an increase of BSA-FITC uptake in monocytes (Figure 3.7D), however PCL/CHI NPs still seem to be the ones that lead to the higher increase (Figure 3.7E). We can speculate that this higher ability of PCL/CHI NPs is related to the presence of CHI and to its positive charges (Sreekumar, S. *et al.*, 2018) that have an improved interaction with the cell negative charges (Ma, Y. *et al.*, 2017). All in considered, these different images of confocal microscopy confirmed the results and conclusions discussed above.

3.2.5 PLA NPs are less cytotoxic than PCL based nanoparticles in RAW 264.7 cell line

Similarly to the cell viability experiments conducted in PBMCs, MTT assay was used to evaluate the cytotoxicity of different NPs after 24 h incubation with the macrophage RAW 264.7 cell line. Results are presented in Figure 3.8.

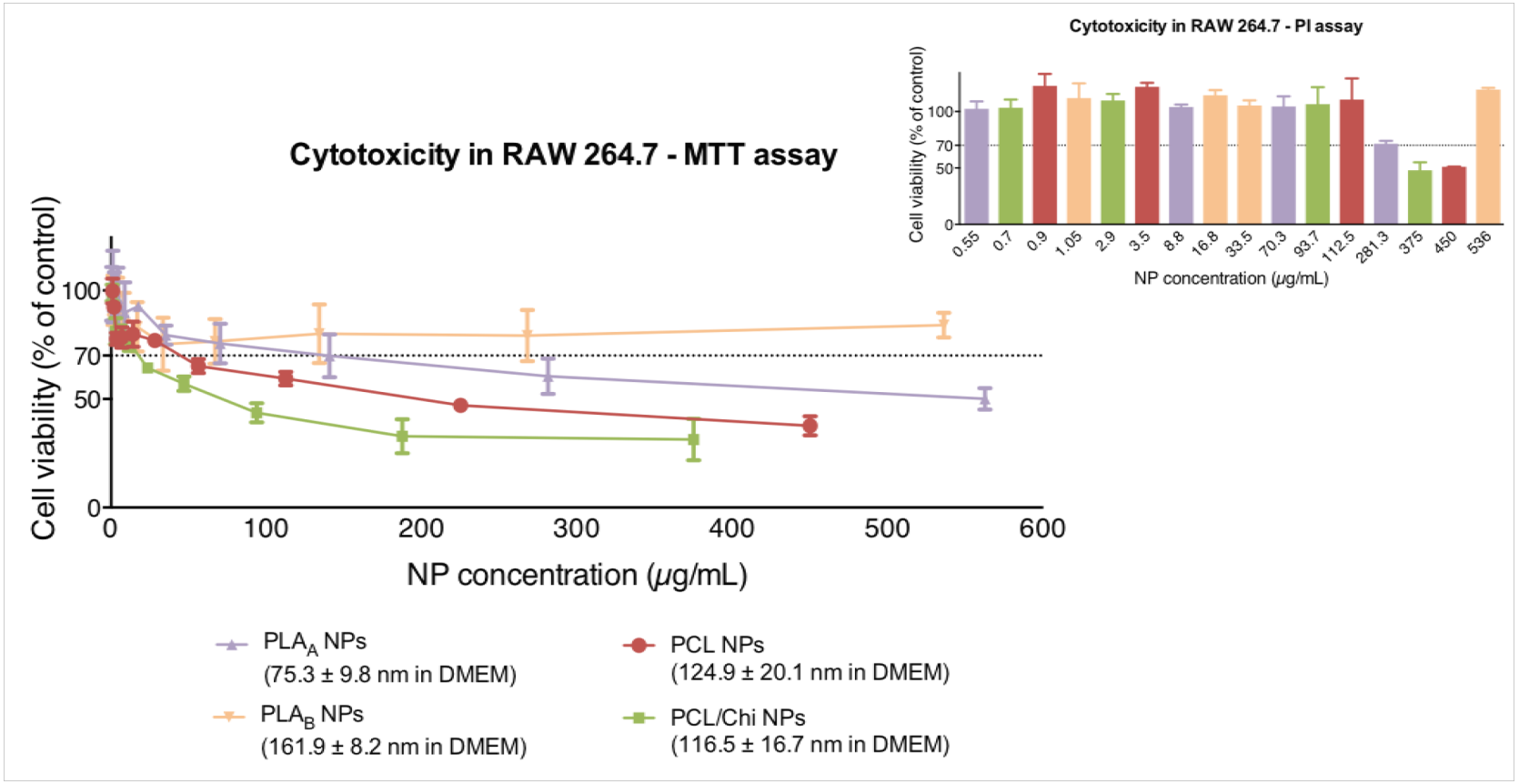

Figure 3. 8 – Cytotoxicity assays (MTT and PI), performed in RAW 264.7 macrophage cell line after 24 h of incubation with different NPs. Data are presented as mean ± SEM, n≥4 (four or more independent experiments, each in triplicate).

Concerning cytotoxicity in RAW 264.7, we can observe in Figure 3.8 that PLA_A NPs presented a higher cytotoxicity than PLA_B NPs. In fact, PLA_A NPs presented an estimated IC_{50} of 540.6 µg/mL, while with PLA_B NPs cell viabilities below 70 % were never reached, and therefore the estimation of IC_{50} was not possible under the concentration range tested (1.05 µg/mL to 536 µg/mL). These results may be explained by the different characteristics of the PLA NPs when placed in contact with cells. In fact, PLA NPs with the smaller size in DMEM medium (PLA_A NPs) were the ones who induced the higher cytotoxicity.

However, when comparing these results with the ones obtained for PCL and PCL/CHI NPs, we can see that PCL/CHI NPs were the more toxic NPs, since they presented an estimated IC_{50} of 68.89 µg/mL. Besides that, PCL NPs presented an estimated IC_{50} of 195.1 µg/mL, which is still more toxic than both PLA NPs.

In order to avoid possible excessive assumption regarding cytotoxicity when using only a metabolic assay, these results were confirmed, here again, with PI assay, which evaluates the integrity of the cell membrane. Results were similar to the ones obtained with MTT (Figure 3.8).

One of the most important conclusions herein presented is that even small changes in the physicochemical characteristics of similar NPs (like the size) can originate different cytotoxicity profiles. In detail, results from RAW 264.7 suggested that PLA_A NPs induced the higher toxicity when compared to PLA_B NPs, and data from the NP characterization in the experiment conditions (Figure 2.5 from Chapter 2) revealed these NPs presented the smaller mean diameter, resultant from a higher heterogeneity of the NP population, with emphasize for a population presenting a mean diameter of 10 nm. Considering these results, we can hypothesize that the smaller NP population in PLA_A NPs, resultant from a modification after dispersion in cell culture medium, is contributing to an increased toxicity of PLA NPs. These results are concordant with the concept that smaller NP can induce more cellular damages, due to increased ability to enter the cells, and particularly, sizes < 10 nm can even reach the cell nucleus (Sukhanova, A. *et al.*, 2018).

Additionally, it is important to highlight that in general PLA NPs were found to be less toxic than PCL NPs and PCL/CHI NPs. In fact, both PCL NPs and PCL/CHI NPs size distribution when dispersed in DMEM changed in a similar way as PLA_A NPs. In all these NPs a smaller size population with less than 25 nm was evident in the size distribution graphs (Figure 2.5 from Chapter 2) and this can be the cause of the increased cytotoxicity observed. In the case of PCL/CHI NPs, the higher toxicity might also be related with a higher affinity of the NPs with the cellular membranes due to the presence of CHI. The positive charges of the

protonated CHI (Sreekumar, S. *et al.*, 2018) are known to interact with the negative surface charge cell membrane, potentially increasing the cytotoxicity (Ma, Y. *et al.*, 2017). Consequently, we can conclude that both PLA NPs produced within this study presented a reduced cytotoxicity when compared to PCL based NPs in this cell line which is an important insight when applying safe-by-design of drug delivery systems.

3.2.6 PLA_A NPs and PCL/CHI NPs induce a significant concentration-dependent ROS production in RAW 264.7

ROS, such as superoxide or hydrogen peroxide, are continually produced during metabolic processes (Brüne, B. *et al.*, 2013, Kwon, D.H. *et al.*, 2017). ROS generation is normally counterbalanced by the action of antioxidant enzymes and other redox molecules (Brüne, B. *et al.*, 2013, Kwon, D.H. *et al.*, 2017). However, when overproduced by activated macrophages, ROS can lead to cellular injury (Brüne, B. *et al.*, 2013, Circu, M.L. and Aw, T.Y., 2010, Kwon, D.H. *et al.*, 2017). It has been proven by Saini and co-workers that NPs may promote apoptotic cell death, through the induction of oxidative stress by accumulating ROS (Saini, P. *et al.*, 2016). Therefore, it is important to evaluate the potential effect of different NPs in ROS production. This assay was performed using the cell-permeable fluorogenic probe DCFH-DA, which can be detected on a standard fluorometric plate reader (Zolnik, B.Potter, T.M. and Stern, S.T., 2011). ROS production assay in RAW 264.7 was performed after 24 h of incubation with the different NPs. Results are presented in Figure 3.9.

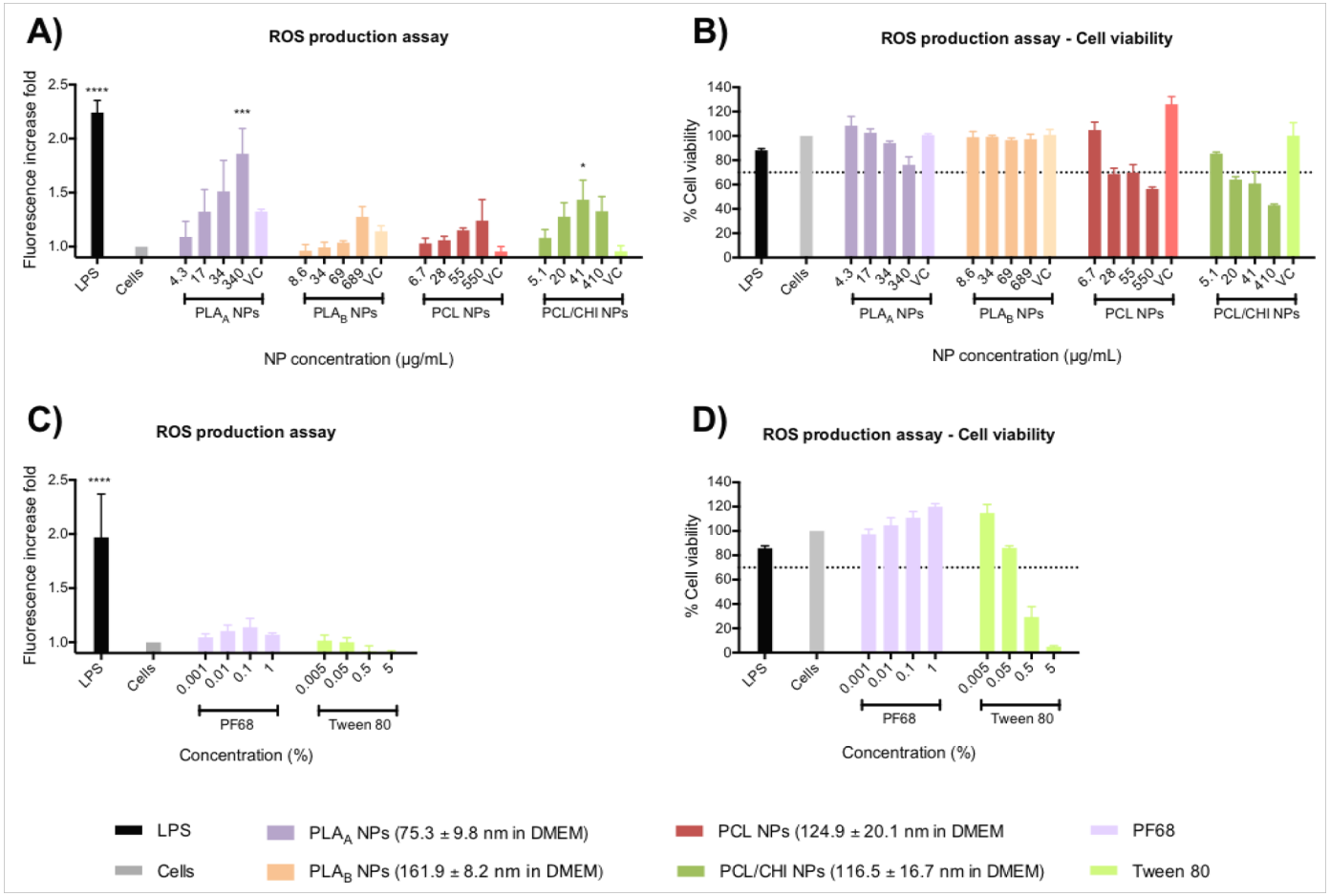

Figure 3. 9 – Generation of reactive oxygen species (ROS) in RAW 264.7 macrophage cell line after 24 h of incubation with NPs and NPs dispersion media (VC). A) ROS production assay using LPS as a positive control and unstimulated cells as a negative control. Results are presented in fluorescence increase fold compared to the negative control. B) Cell viability assay (MTT) after the performance of ROS production assay. C) ROS production assay with surfactants used in the NP preparation, using LPS as a positive control and unstimulated cells as a negative control. Results are presented in fluorescence increase fold compared to the negative control. D) Cell viability assay (MTT) after the performance of ROS production assay with surfactants used in the NP preparation. Data are presented as mean ± SEM, n≥3 (three or more independent experiments, each in triplicate).

As demonstrated in Figure 3.9A, there was a concentration-dependent ROS production for PLA_A NPs even with lower NP concentrations than PLA_B NPs (4.3 µg/mL to 340 µg/mL for PLA_A NPs and 8.6 µg/mL to 690 µg/mL for PLA_B NPs). We could hypothesize that this concentration-dependent ROS production is an indication of cellular toxicity, as demonstrated by the cell viability assay in the Figure 3.9B, where for the higher PLA_A NP concentration the resultant cellular viability was near 70 %. For PLA_B NPs the increase of ROS production was not statistically different from the unstimulated cells (Figure 3.9A). Furthermore, in opposition to the results of PLA_A NPs, no trend for decrease in cell viability was shown for PLA_B NPs (Figure 3.9B). When comparing these results with the ones obtained for PCL and PCL/CHI NPs, a concentration-dependent ROS production was also observable for both NPs, however, only statistically different from the unstimulated cells for PCL/CHI NPs (Figure 3.9A). This result suggests that the presence of CHI in the NPs exacerbated their effect on ROS production. Here again we can corelate the concentration-dependent ROS production to the cellular toxicity, since for higher NP concentration there was a significant decrease of cell viability (< 70%) (Figure 3.9B). Importantly, in the case of PCL/CHI NPs the highest ROS production was not induced by the highest concentration. We can hypothesize that since this concentration caused a decrease of cell viability to values below 50 %, probably other mechanisms of cell death were associated, reducing the number of cells producing ROS.

We also hypothesized that particularly for PLA NPs the amount of surfactant could be responsible for the concentration-dependent ROS production, because PLA_A NPs were produced in the presence of higher surfactant amount. However, this fact was not confirmed, since we tested PF68 and Tween 80 and neither induced ROS production under the concentration-range tested (0.001 % to 1% for PF68 and 0.005 % to 5% for Tween 80) (Figure 3.9C). To highlight, none of the percentages of PF68 induced cellular toxicity, contrary to the higher percentages of Tween 80 that lead to a high cellular death. Despite most of the surfactants are eliminated by the NP washing steps, we can speculate that some surfactant may still be present and also contribute to the cellular toxicity of PCL and PCL/CHI NPs (Figure 3.9D).

To summarize, we demonstrated that PLA_A NPs induced a concentration-dependent ROS production, whereas PLA_B NPs did not stimulate statistically significant ROS production even with higher concentrations. A published report from Singh and co-workers (Singh, R.P. and Ramarao, P., 2013) suggested that PLA NPs (emulsion-diffusion-evaporation method using PVA) is not able to induce ROS production up to 100 µg/mL concentration, whereas 300 µg/mL showed 1.5- to 2-fold stimulation of ROS production. Their results are in agreement

with ours for PLA_A NPs, however, they are not aligned with the results from PLA_B NPs. This stresses the importance of an adequate evaluation when testing distinct polymeric nanomaterials rather than excessively extrapolating conclusions. Interestingly, Singh and Ramarao demonstrated a 1.5- to 2-fold stimulation of ROS production with PCL NPs at 300 µg/mL (Singh, R.P. and Ramarao, P., 2013), which is contradictory with our results. In fact, PCL NPs produced within this study did not stimulate a statistically significant ROS production even with 500 µg/mL. In our study, only PCL/CHI NPs induced ROS production with statistical significance at a concentration much lower than 300 µg/mL (41 µg/mL), which can be related to CHI presence in the NPs. From our research in the literature, we did not find any article studying the effect of PCL/CHI NPs on ROS production, however, some articles correlated the influence of CHI NPs on ROS production but with several controversies. In fact, some of them observed a concentration-dependent ROS production induced by CHI NPs at concentrations from 10 µg/mL to 100 µg/mL (Sarangapani, S. *et al.*, 2018, Wang, H. *et al.*, 2018), which is in agreement with our results, but others reported no effect of CHI NPs on ROS production from 100 µg/mL to 1000 µg/mL (Arora, D. *et al.*, 2016a, Omar, S.S., Katas, H. and Hamid, Z.A., 2015). Still, it is important to highlight that the experimental conditions used in the articles differ from each other and, thus, it must be emphasized, once more, that there is an essential need to standardize the procedures.

3.2.7 None of the developed polyester NPs induced NO production in RAW 264.7

NO is a reactive nitrogen species produced by nitric oxide synthase enzymes (Bosca, L. *et al.*, 2005, Caruso, G. *et al.*, 2017). It is an important inflammatory mediator released by macrophages during inflammation, and is one of the main cytostatic, cytotoxic, and pro-apoptotic mechanisms of the immune response (Bosca, L. *et al.*, 2005, Caruso, G. *et al.*, 2017). In order to assess the potential inflammatory or anti-inflammatory properties of PLA NPs, NO production by RAW 264.7 cells was measured using the Griess reaction method after 24 h incubation with different test samples.

The pro-inflammatory effect of NPs was evaluated by measuring the NO release upon stimulation with different NPs, and the anti-inflammatory effect was evaluated by measuring the ability of the NPs to inhibit NO release from cells previously stimulated with LPS stimulus. Results are presented in Figure 3.10.

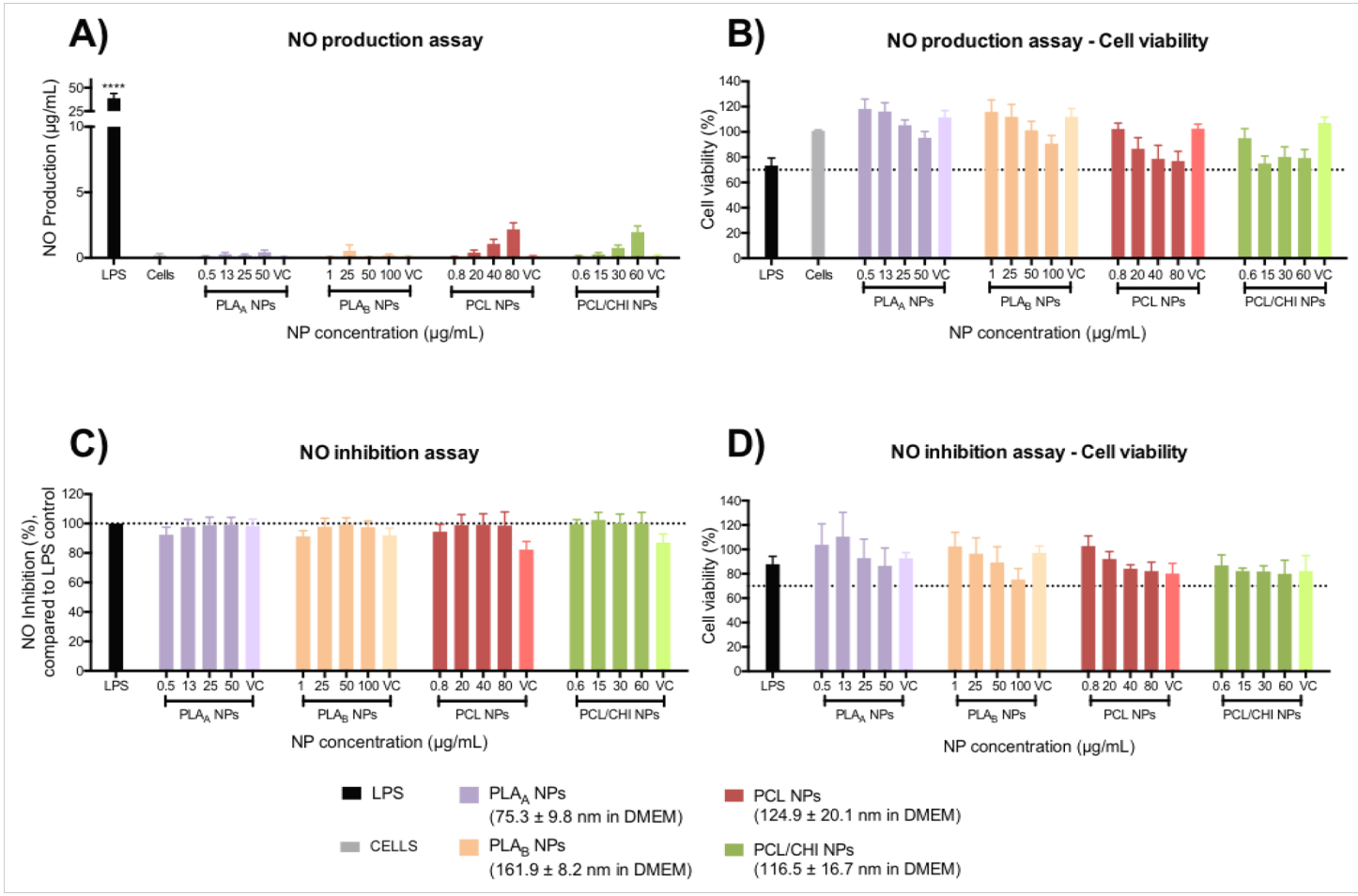

Figure 3. 10 – Production of NO by RAW 264.7 macrophage cell line after 24 h incubation with NPs and NPs dispersion media (VC). A) NO production assay using LPS as a positive control and unstimulated cells as a negative control. B) Cell viability assay (MTT) after the evaluation of the NO production. C) NO inhibition assay. For the estimation of NPs inhibitory effect on NO production, NPs were incubated simultaneously with LPS. The percentage of NO inhibition was calculated considering 100 % the NO production induced by LPS without NPs. D) Cell viability assay (MTT) after the evaluation of the NO. Data are presented as mean ± SEM, n≥3 (three or more independent experiments, each in triplicate).

It was possible to observe that none of the NPs induced a significant NO production under the concentration range tested (0.5 µg/mL to 50 µg/mL for PLA_A NPs; 1 µg/mL to 100 µg/mL for PLA_B NPs; 0.8 µg/mL to 80 µg/mL for PCL NPs; 0.6 µg/mL to 60 µg/mL for PCL/CHI NPs) (Figure 3.10A). Although there were no significant differences, it must be underlined that PCL and PCL/CHI NPs showed a tendency to induce a concentration-dependent NO production. Importantly, these concentrations were chosen because they did not induce significant cellular death under the assay conditions, and higher concentrations would result in cellular death above 30 %, which could compromise NO production (Figure 3.10B).

When using the same concentration ranges, the second approach, which evaluate the anti-inflammatory effect, revealed that all non-cytotoxic concentrations (Figure 3.10D) of NPs under test did not inhibited the NO production previously stimulated with LPS (Figure 3.10C). Additionally, it must be noted that the VC of PCL and PCL/CHI NPs seemed to slightly inhibit NO production, although without significant differences from negative control (LPS). A hypothesis to explain that result could be related with the presence of smaller NPs in the supernatant, explaining both, the decrease of cell viability and NO production observed for VC.

According to literature, PLA may induce inflammatory responses, due to its hydrophobicity, lack of bioactivity, and release of acidic degradation by-products (Farah, S., Anderson, D.G. and Langer, R., 2016, Li, H. and Chang, J., 2004, Yoon, S.-D., Kwon, Y.-S. and Lee, K.-S., 2017). Nevertheless, this study showed that PLA polymer properties are not fully exchangeable with nanosized PLA particles. Actually, we showed that both PLA NPs produced within this study did not present effects on NO production under the concentration range tested, suggesting it does not induce an inflammatory response in the macrophage RAW 264.7 cell line. Regarding PCL and CHI polymers, they also may induce inflammatory responses according to Corradetti (Corradetti, B., 2017). However, as demonstrated in this study, neither PCL nor PCL/CHI NPs produced within this study presented effects on NO production with statistical significance under the concentration range tested, hypothesizing both do not induce an inflammatory response in the macrophage RAW 264.7 cell line.

Chapter 4 – Concluding remarks and future perspectives

PLA is being widely studied for biomedical applications as a nanoparticulate drug delivery system, however, not much work has been published regarding its immunotoxicity and even some inconsistent results between authors can be found.

Accordingly, one of the major aims of this study was to develop and optimize two different methods to produce two different sized PLA NPs and to perform a broad NPs characterization in pyrogen-free water as well as in the different cell culture media used. This aim was achieved by a simple nanoprecipitation method, which allowed us to obtain two different sized PLA NPs: PLA_A NPs with 187.9 nm $\pm$ 36.9 nm and PLA_B NPS with 109.1 nm $\pm$ 10.4 nm, both dispersed in pyrogen-free water. With these NPs (PLA_A and PLA_B NPs), we also aimed to study the effect of the size on the immunotoxicological properties of PLA NPs. Besides these two NPs, two other polymeric NPs were prepared by the optimization of a method previously developed by our laboratory. From this second optimization, we obtained PCL NPs with 170.0 nm $\pm$ 15.2 nm and PCL/CHI NPs with 266.1 nm $\pm$ 63.8 nm, which were used to study the effect of the presence of CHI on the NP structure and also to compare with PLA NPs. However, we demonstrated that the NPs physicochemical properties were altered after the dispersion in cell culture media and probably this had repercussions on the immunotoxicological profile of each NP. As a consequence, another major aim had arisen, consisting on the evaluation of the immunotoxicological effects of each NP and on the association with the respective NP characterization in the assay experimental conditions. The hypothesis that smaller NPs were able to induce higher cellular toxicity and ROS production was possible only by addressing the results from the characterization in cell culture media. These results illustrate how an adequate NP characterization is crucial and can avoid misinterpretations and ambiguous conclusions. Importantly, this adequate characterization in *in vitro* assay conditions can be further transposable to *in vivo* conditions. In fact, the contact of the NPs with biological solutions, such as blood, saliva, nasal or gastric fluids is known to be essential for the generation of a biological effect, however it can have repercussions on the NPs physicochemical properties (Park, J.H. and Oh, N., 2014).

Taking into account the results from the different assays performed, we can conclude that both PLA NPs presented a safer immunotoxicity profile compared with PCL NPs and PCL/CHI NPs, which reinforced their promising application as delivery systems. Moreover, the presence of CHI in the PCL-based NPs was proved to be linked with more immunotoxicological effects. However, the presence of CHI also proved to be linked with a better BSA adsorption and uptake by PBMCs. Therefore, all the pros and cons of the presence of CHI in the NP structure have to be considered for the determination of the most suitable nanoparticulate delivery system for a specific therapeutic application.

All in considered, I strongly believe that all the initially proposed objectives were achieved. These results contribute to the current scientific evidence, and also alert other researchers for the importance of the formulations physicochemical characterization.

In the future, some results could be confirmed using other methodologies to increase the robustness of the conclusions. For instance, hemocompatibility could be further evaluated by testing coagulation times and platelet aggregation upon contact with these NPs. Similarly, other cytokines release could be tested, such as IFN-γ (pro-inflammatory) or IL-10 (immunosuppressive), and also new controls using polymyxin B to avoid any interference from endotoxin contamination, even though the NPs were produced in LPS-free conditions.

Chapter 5 – References

ALTMEYER, C., *et al.* - Tamoxifen-loaded poly(L-lactide) nanoparticles: Development, characterization and in vitro evaluation of cytotoxicity. **Materials Science and Engineering: C**. Vol. 60 (2016) p. 135-142. ISSN:09284931. DOI:10.1016/j.msec.2015.11.019.

ARANGO, G.; DESCOTEAUX, A. - Macrophage cytokines: involvement in immunity and infectious diseases. **Front Immunol**. Vol. 5 (2014) p. 491. ISSN:1664-3224. DOI:10.3389/fimmu.2014.00491.

ARORA, D., *et al.* - Preparation, characterization and toxicological investigation of copper loaded chitosan nanoparticles in human embryonic kidney HEK-293 cells. **Mater Sci Eng C Mater Biol Appl**. Vol. 61 (2016a) p. 227-34. ISSN:1873-0191. DOI:10.1016/j.msec.2015.12.035.

ARORA, D., *et al.* - Preparation, characterization and toxicological investigation of copper loaded chitosan nanoparticles in human embryonic kidney HEK-293 cells. **Materials Science and Engineering: C**. Vol. 61 (2016b) p. 227-234. ISSN:09284931. DOI:10.1016/j.msec.2015.12.035.

ASTM - ASTM E2524-08(2013) - Standard Test Method for Analysis of Hemolytic Properties of Nanoparticles. West Conshohocken, PA: **ASTM International**, 2013. Consult. em 26.09.18. Available at: https://www.astm.org/Standards/E2524.htm. ISBN/ISSN:

BEHZADI, S., *et al.* - Cellular uptake of nanoparticles: journey inside the cell. **Chem Soc Rev**. Vol. 46 (2017) p. 4218-4244. ISSN:1460-4744. DOI:10.1039/c6cs00636a.

BOSCA, L., *et al.* - Nitric oxide and cell viability in inflammatory cells: a role for NO in macrophage function and fate. **Toxicology**. Vol. 208 (2005) p. 249-258. ISSN:0300483X. DOI:10.1016/j.tox.2004.11.035.

BOSHTAM, M., *et al.* - Aptamers Against Pro- and Anti-Inflammatory Cytokines: A Review. **Inflammation**. Vol. 40 (2017) p. 340-349. ISSN:1573-2576. DOI:10.1007/s10753-016-0477-1.

BRÜNE, B., *et al.* - Redox Control of Inflammation in Macrophages. **Antioxidants & Redox Signaling**. Vol. 19 (2013) p. 595-637. ISSN:1523-0864. DOI:10.1089/ars.2012.4785.

CAI, X., *et al.* - Inflammatory factor TNF-alpha promotes the growth of breast cancer via the positive feedback loop of TNFR1/NF-kappaB (and/or p38)/p-STAT3/HBXIP/TNFR1.

Oncotarget. Vol. 8 (2017) p. 58338-58352. ISSN:1949-2553. DOI:10.18632/oncotarget.16873.

CARUSO, G.*, et al.* - Carnosine modulates nitric oxide in stimulated murine RAW 264.7 macrophages. **Molecular and Cellular Biochemistry**. Vol. 431 (2017) p. 197-210. ISSN:0300-8177. DOI:10.1007/s11010-017-2991-3.

CASTRO-AGUIRRE, E.; KUMAR, A. - Nanoparticles in Drug Delivery Systems. **Nanomedicine in Drug Delivery.** (2013). ISBN: 978-1-4665-0616-9. DOI: 10.1201/b14802-2.

CASTRO-AGUIRRE, E.*, et al.* - Poly(lactic acid)-Mass production, processing, industrial applications, and end of life. **Adv Drug Deliv Rev**. Vol. 107 (2016) p. 333-366. ISSN:1872-8294. DOI:10.1016/j.addr.2016.03.010.

CIRCU, M. L.; AW, T. Y. - Reactive oxygen species, cellular redox systems, and apoptosis. **Free Radical Biology and Medicine**. Vol. 48 (2010) p. 749-762. ISSN:08915849. DOI:10.1016/j.freeradbiomed.2009.12.022.

CORRADETTI, B. - The Immune Response to Implanted Materials and Devices. **Springer Nature**, 2017. ISBN: 978-3-319-45433-7

DA SILVA, J.*, et al.* - Poly(D,L-Lactic Acid) Nanoparticle Size Reduction Increases Its Immunotoxicity. **Frontiers in Bioengineering and Biotechnology**. Vol. 7 (2019) ISSN:2296-4185. DOI:10.3389/fbioe.2019.00137.

DE FARIA, T. J.; DE CAMPOS, A.; LEMOS, E. - Preparation and Characterization of Poly(D,L-Lactide) (PLA) and Poly(D,L-Lactide)-Poly(Ethylene Glycol) (PLA-PEG) Nanocapsules Containing Antitumoral Agent Methotrexate. **Macromolecular Symposia**. Vol. 229 (2005) p. 228-233. ISSN:1022-1360. DOI:10.1002/masy.200551128.

DOBROVOLSKAIA, M. A.; MCNEIL, S. E. - Immunological properties of engineered nanomaterials. **Nat Nanotechnol**. Vol. 2 (2007) p. 469-78. ISSN:1748-3395. DOI:10.1038/nnano.2007.223.

DOBROVOLSKAIA, M. A.*, et al.* - Method for Analysis of Nanoparticle Hemolytic Properties in Vitro. **Nano Letters**. Vol. 8 (2008) p. 2180-2187. ISSN:1530-6984. DOI:10.1021/nl0805615.

DOBROVOLSKAIA, M. A.; McNeil, Scott E. - Understanding the correlation between in vitro and in vivo immunotoxicity tests for nanomedicines. **Journal of Controlled Release**. Vol. 172 (2013) p. 456-466. ISSN:01683659. DOI:10.1016/j.jconrel.2013.05.025.

EMEA - Reflection paper on nanotechnology-based medicinal products for human use (EMEA/CHMP/79769/2006). (2006).

EUROPEAN PHARMACOPEIA - Reverse osmosis in Ph. Eur. monograph - water for injections (0169). **European Pharmacopoeia**. (2016).

FARAH, S.; ANDERSON, D. G.; LANGER, R. - Physical and mechanical properties of PLA, and their functions in widespread applications — A comprehensive review. **Advanced Drug Delivery Reviews**. Vol. 107 (2016) p. 367-392. ISSN:0169409X. DOI:10.1016/j.addr.2016.06.012.

FDA - Considering Whether an FDA-Regulated Product Involves the Application of Nanotechnology (FDA-2010-D-0530). (2014).

FESSI, H., *et al.* - Nanocapsule formation by interfacial polymer deposition following solvent displacement. **International Journal of Pharmaceutics**. Vol. 55 (1989) p. R1-R4. ISSN:03785173. DOI:10.1016/0378-5173(89)90281-0.

FUOCO, T.; FINNE-WISTRAND, A. - Enhancing the Properties of Poly(epsilon-caprolactone) by Simple and Effective Random Copolymerization of epsilon-Caprolactone with p-Dioxanone. **Biomacromolecules**. (2019) ISSN:1526-4602. DOI:10.1021/acs.biomac.9b00745.

GRABOWSKI, N., *et al.* - Surface coating mediates the toxicity of polymeric nanoparticles towards human-like macrophages. **Int J Pharm**. Vol. 482 (2015) p. 75-83. ISSN:1873-3476. DOI:10.1016/j.ijpharm.2014.11.042.

GRABOWSKI, N., *et al.* - Surface-Modified Biodegradable Nanoparticles' Impact on Cytotoxicity and Inflammation Response on a Co-Culture of Lung Epithelial Cells and Human-Like Macrophages. **Journal of Biomedical Nanotechnology**. Vol. 12 (2016) p. 135-146. ISSN:15507033. DOI:10.1166/jbn.2016.2126.

GUPTA, B.; REVAGADE, N.; HILBORN, J. - Poly(lactic acid) fiber: An overview. **Progress in Polymer Science**. Vol. 32 (2007) p. 455-482. ISSN:00796700. DOI:10.1016/j.progpolymsci.2007.01.005.

HIRSJÄRVI, S. - Preparation and Characterization of Poly(Lactic Acid) Nanoparticles for Pharmaceutical Use. **University of Helsinki Finland**, 2008.

ILLUM, L., *et al.* - Chitosan as a novel nasal delivery system for vaccines. **Advanced Drug Delivery Reviews**. Vol. 51 (2001) p. 81-96. ISSN:0169409X. DOI:10.1016/s0169-409x(01)00171-5.

ISO - Biological evaluation of medical devices. **International Organization for Standardization**. (2018).

ISO/TC229 - ISO/TS 80004-1:2015 - Nanotechnologies -- Vocabulary -- Part 1: Core terms. **International Organization for Standardization**. (2015a) p. 3.

ISO/TC229 - ISO/TS 80004-2:2015 - Nanotechnologies -- Vocabulary -- Part 2: Nano-objects. **International Organization for Standardization**. (2015b) p. 10.

JESUS, S., *et al.* - The Inclusion of Chitosan in Poly-epsilon-caprolactone Nanoparticles: Impact on the Delivery System Characteristics and on the Adsorbed Ovalbumin Secondary Structure. **AAPS PharmSciTech**. Vol. 19 (2018) p. 101-113. ISSN:1530-9932. DOI:10.1208/s12249-017-0822-1.

JESUS, S.; SOARES, E.; BORGES, O. - Poly-epsilon-caprolactone/Chitosan and Chitosan Particles: Two Recombinant Antigen Delivery Systems for Intranasal Vaccination. **Methods Mol Biol**. Vol. 1404 (2016) p. 697-713. ISSN:1940-6029. DOI:10.1007/978-1-4939-3389-1_45.

JESUS, S., *et al.* - Adjuvant Activity of Poly-ε-caprolactone/Chitosan Nanoparticles Characterized by Mast Cell Activation and IFN-γ and IL-17 Production. **Molecular Pharmaceutics**. Vol. 15 (2017) p. 72-82. ISSN:1543-8384. DOI:10.1021/acs.molpharmaceut.7b00730.

KARCHIYAPPAN, T.; PRASAD, R. - Advanced Research in Nanosciences for Water Technology. Springer, 2019.

KONONENKO, V.; NARAT, M.; DROBNE, D. - Nanoparticle interaction with the immune system. **Arh Hig Rada Toksikol**. Vol. 66 (2015) p. 97-108. ISSN:1848-6312. DOI:10.1515/aiht-2015-66-2582.

KULKARNI, A. D., *et al.* - N,N,N-Trimethyl chitosan: An advanced polymer with myriad of opportunities in nanomedicine. **Carbohydr Polym**. Vol. 157 (2017) p. 875-902. ISSN:1879-1344. DOI:10.1016/j.carbpol.2016.10.041.

KWON, D. H., *et al.* - Inhibitory effects on the production of inflammatory mediators and reactive oxygen species by Mori folium in lipopolysaccharide-stimulated macrophages and zebrafish. **Anais da Academia Brasileira de Ciências**. Vol. 89 (2017) p. 661-674. ISSN:0001-3765. DOI:10.1590/0001-3765201720160836.

LABET, M.; THIELEMANS, W. - Synthesis of polycaprolactone: a review. **Chem Soc Rev**. Vol. 38 (2009) p. 3484-504. ISSN:1460-4744. DOI:10.1039/b820162p.

LASPRILLA, J., *et al.* - Synthesis and Characterization of Poly (Lactic Acid) for Use in Biomedical Field. 2011.

LAVERTU, M., *et al.* - A validated 1H NMR method for the determination of the degree of deacetylation of chitosan. **Journal of Pharmaceutical and Biomedical Analysis**. Vol. 32 (2003) p. 1149-1158. ISSN:07317085. DOI:10.1016/s0731-7085(03)00155-9.

LEGAZ, S., *et al.* - Evaluation of polylactic acid nanoparticles safety using Drosophila model. **Nanotoxicology**. Vol. 10 (2016) p. 1136-1143. ISSN:1743-5390. DOI:10.1080/17435390.2016.1181806.

LI, H.; CHANG, J. - Preparation and characterization of bioactive and biodegradable Wollastonite/poly(D,L-lactic acid) composite scaffolds. **Journal of Materials Science: Materials in Medicine**. Vol. 15 (2004) p. 1089-1095. ISSN:0957-4530. DOI:10.1023/B:JMSM.0000046390.09540.c2.

MA, Y., *et al.* - Introducing Membrane Charge and Membrane Potential to T Cell Signaling. **Front Immunol**. Vol. 8 (2017) p. 1513. ISSN:1664-3224. DOI:10.3389/fimmu.2017.01513.

MOHAN, M. L.; VASUDEVAN, N. T.; NAGA PRASAD, S. V. - Proinflammatory Cytokines Mediate GPCR Dysfunction. **J Cardiovasc Pharmacol**. Vol. 70 (2017) p. 61-73. ISSN:1533-4023. DOI:10.1097/FJC.0000000000000456.

MOORKOTH, D.; NAMPOOTHIRI, K. M. - Synthesis, colloidal properties and cytotoxicity of biopolymer nanoparticles. **Appl Biochem Biotechnol**. Vol. 174 (2014) p. 2181-94. ISSN:1559-0291. DOI:10.1007/s12010-014-1172-z.

MURARIU, M.; DUBOIS, P. - PLA composites: From production to properties. **Adv Drug Deliv Rev**. Vol. 107 (2016) p. 17-46. ISSN:1872-8294. DOI:10.1016/j.addr.2016.04.003.

MUXIKA, A., *et al.* - Chitosan as a bioactive polymer: Processing, properties and applications. **Int J Biol Macromol**. Vol. 105 (2017) p. 1358-1368. ISSN:1879-0003. DOI:10.1016/j.ijbiomac.2017.07.087.

NAIR, L. S.; LAURENCIN, C. T. - Biodegradable polymers as biomaterials. **Progress in Polymer Science**. Vol. 32 (2007) p. 762-798. ISSN:00796700. DOI:10.1016/j.progpolymsci.2007.05.017.

OMAR, S. S.; KATAS, H.; HAMID, Z. - Lineage-related and particle size-dependent cytotoxicity of chitosan nanoparticles on mouse bone marrow-derived hematopoietic stem and progenitor cells. **Food and Chemical Toxicology**. Vol. 85 (2015) p. 31-44. ISSN:02786915. DOI:10.1016/j.fct.2015.05.017.

PANDEY, S. K., *et al.* - Anti-cancer evaluation of quercetin embedded PLA nanoparticles synthesized by emulsified nanoprecipitation. **Int J Biol Macromol**. Vol. 75 (2015) p. 521-9. ISSN:1879-0003. DOI:10.1016/j.ijbiomac.2015.02.011.

PARIHAR, A.; EUBANK, T. D.; DOSEFF, A. I. - Monocytes and macrophages regulate immunity through dynamic networks of survival and cell death. **J Innate Immun**. Vol. 2 (2010) p. 204-15. ISSN:1662-8128. DOI:10.1159/000296507.

PARK, J. H.; OH, N. - Endocytosis and exocytosis of nanoparticles in mammalian cells. **International Journal of Nanomedicine**. (2014) p. 51. ISSN:1178-2013. DOI:10.2147/ijn.s26592.

PATTANI, A., *et al.* - Immunological Effects and Membrane Interactions of Chitosan Nanoparticles. **Molecular Pharmaceutics**. Vol. 6 (2009) p. 345-352. ISSN:1543-8384. DOI:10.1021/mp900004b.

SAINI, P., *et al.* - Evidence of reactive oxygen species (ROS) mediated apoptosis in Setaria cervi induced by green silver nanoparticles from Acacia auriculiformis at a very low dose. **Experimental Parasitology**. Vol. 160 (2016) p. 39-48. ISSN:00144894. DOI:10.1016/j.exppara.2015.11.004.

SALGIN, S.; SALGIN, U.; BAHADIR, S. - Zeta Potentials and Isoelectric Points of Biomolecules: The Effects of Ion Types and Ionic Strengths. **International Journal of Electrochemical Science**. Vol. 7 (2012).

SAMBANDAM, B., *et al.* - Synthesis and characterization of poly D-L lactide (PLA) nanoparticles for the delivery of quercetin. 2015.

SANTANDER-ORTEGA, M. J., *et al.* - Colloidal stability of Pluronic F68-coated PLGA nanoparticles: A variety of stabilisation mechanisms. **Journal of Colloid and Interface Science**. Vol. 302 (2006) p. 522-529. ISSN:00219797. DOI:10.1016/j.jcis.2006.07.031.

SARANGAPANI, S., *et al.* - Chitosan nanoparticles' functionality as redox active drugs through cytotoxicity, radical scavenging and cellular behaviour. **Integrative Biology**. Vol. 10 (2018) p. 313-324. ISSN:1757-9694. DOI:10.1039/c8ib00038g.

SHELMA, R.; SHARMA, C. P. - Development of lauroyl sulfated chitosan for enhancing hemocompatibility of chitosan. **Colloids and Surfaces B: Biointerfaces**. Vol. 84 (2011) p. 561-570. ISSN:09277765. DOI:10.1016/j.colsurfb.2011.02.018.

SINGH, R.; RAMARAO, P. - Accumulated Polymer Degradation Products as Effector Molecules in Cytotoxicity of Polymeric Nanoparticles. **Toxicological Sciences**. Vol. 136 (2013) p. 131-143. ISSN:1096-6080. DOI:10.1093/toxsci/kft179.

SREEKUMAR, S., *et al.* - Parameters influencing the size of chitosan-TPP nano- and microparticles. **Sci Rep**. Vol. 8 (2018) p. 4695. ISSN:2045-2322. DOI:10.1038/s41598-018-23064-4.

SUKHANOVA, A., *et al.* - Dependence of Nanoparticle Toxicity on Their Physical and Chemical Properties. **Nanoscale Res Lett**. Vol. 13 (2018) p. 44. ISSN:1931-7573. DOI:10.1186/s11671-018-2457-x.

TSUJI, H. - Poly(lactic acid) stereocomplexes: A decade of progress. **Adv Drug Deliv Rev**. Vol. 107 (2016) p. 97-135. ISSN:1872-8294. DOI:10.1016/j.addr.2016.04.017.

TYLER, B., *et al.* - Polylactic acid (PLA) controlled delivery carriers for biomedical applications. **Adv Drug Deliv Rev**. Vol. 107 (2016) p. 163-175. ISSN:1872-8294. DOI:10.1016/j.addr.2016.06.018.

VILLIERS, C., *et al.* - From Secretome Analysis to Immunology. **Molecular & Cellular Proteomics**. Vol. 8 (2009) p. 1252-1264. ISSN:1535-9476. DOI:10.1074/mcp.M800589-MCP200.

WANG, H., *et al.* - Chitosan nanoparticles triggered the induction of ROS-mediated cytoprotective autophagy in cancer cells. **Artif Cells Nanomed Biotechnol**. Vol. 46 (2018) p. 293-301. ISSN:2169-141X. DOI:10.1080/21691401.2017.1423494.

WANG, Q., *et al.* - Preparation, blood coagulation and cell compatibility evaluation of chitosan-graft-polylactide copolymers. **Biomed Mater**. Vol. 9 (2014) p. 015007. ISSN:1748-605X. DOI:10.1088/1748-6041/9/1/015007.

WICHRESEARCHLAB - Size-comparison-Bio-nanoparticles nanometer scale comparison nanoparticle size comparison nanotechnology chart ruler. 2017. Available at: https://www.wichlab.com/nanometer-scale-comparison-nanoparticle-size-comparison-nanotechnology-chart-ruler-2/

WOODRUFF, M. A.; HUTMACHER, D. W. - The return of a forgotten polymer—Polycaprolactone in the 21st century. **Progress in Polymer Science**. Vol. 35 (2010) p. 1217-1256. ISSN:00796700. DOI:10.1016/j.progpolymsci.2010.04.002.

YOON, S.D.; KWON, Y.S.; LEE, K.S. - Biodegradation and Biocompatibility of Poly L-lactic Acid Implantable Mesh. **International Neurourology Journal**. Vol. 21 (2017) p. S48-54. ISSN:2093-6931. DOI:10.5213/inj.1734882.441.

YOUNG, S. H., *et al.* - Molecular mechanism of tumor necrosis factor-alpha production in 1->3-beta-glucan (zymosan)-activated macrophages. **J Biol Chem**. Vol. 276 (2001) p. 20781-7. ISSN:0021-9258. DOI:10.1074/jbc.M101111200.

ZOLNIK, B.; POTTER, T. M.; STERN, S. T. - Characterization of Nanoparticles Intended for Drug Delivery. 2011. Cap. Chapter 18 - Detecting Reactive Oxygen Species in Primary Hepatocytes Treated with Nanoparticles. ISBN: 978-1-60327-197-4.